

# A new type of integral bridge comprising geosynthetic-reinforced soil walls

F. Tatsuoka<sup>1</sup>, D. Hirakawa<sup>2</sup>, M. Nojiri<sup>3</sup>, H. Aizawa<sup>4</sup>, H. Nishikiori<sup>5</sup>, R. Soma<sup>6</sup>, M. Tateyama<sup>7</sup> and K. Watanabe<sup>8</sup>

<sup>1</sup>Professor, Department of Civil Engineering, Tokyo University of Science, 2641 Yamazaki, Noda, Chiba, 278-8510, Japan, Telephone: +81 4 7122 9819, Telefax: +81 4 7123 9766, E-mail: tatsuoka@rs.noda.tus.ac.jp

<sup>2</sup>Assistant Professor, Department of Civil and Environmental Engineering, National Defence Academy of Japan, 1-10-20 Hashirimizu, Yokosuka, Kanagawa, 239-8686, Japan, Telephone: +81 46 841 3810, Telefax: +81 46 844 5913, E-mail: hirakawa@nda.ac.jp

<sup>3</sup>Engineer, Kawasaki Geological Engineering Co. Ltd, 1-40 Gion-machi, Hakata-ku, Fukuoka, 812-0038, Japan, Telephone: +81 92 271 9201, Telefax: +81 92 271 9209, E-mail: nojirim@kge.co.jp

<sup>4</sup>Engineer, Japan Railway Construction, Transport and Technology Agency, 45-1 Okada, Nakagosyo, Nagano, 380-0936, Japan, Telephone: +81 26 223 9643, Telefax: +81 26 223 9681, E-mail: h.aizawa@jrtr.go.jp

<sup>5</sup>Engineer, Department of Civil Engineering, Ibaraki Prefecture, 978-6 Kasahara, Mito City, Ibaraki Prefecture, Japan, Telephone: +81 29 301 4530, Telefax: +81 29 301 4538, E-mail: h.nishikiori@pref.ibaraki.lg.jp

<sup>6</sup>Graduate Student, Department of Civil Engineering, Tokyo University of Science, 2641 Yamazaki, Noda, Chiba, 278-8510, Japan, Telephone: +81 4 7124 1501, Telefax: +81 4 7123 9766, E-mail: j7608607@ed.noda.tus.ac.jp

<sup>7</sup>Chief, Structural Engineering Division, Railway Technical Research Institute, Japan, 2-8-38, Hikari-cho, Kokubunji City, Tokyo, 185-8540, Japan, Telephone: +81 42 573 7369, Telefax: +81 42 053 7369, E-mail: tate@rtri.or.jp

<sup>8</sup>Assistant Senior Researcher, Foundation and Geotechnical Engineering Structures Technology Division, Railway Technical Research Institute, Japan, 2-8-38, Hikari-cho, Kokubunji City, Tokyo, 185-8540, Japan, Telephone: +81 42 573 7261, Telefax: +81 42 573 7248, E-mail: nabeken@rtri.or.jp

Received 8 June 2008, revised 23 November 2008, accepted 1 December 2008

**ABSTRACT:** Integral bridges, comprising a continuous bridge girder (i.e. deck) integrated to a pair of abutments without using hinged and movable shoes (i.e. bearings), have been constructed to alleviate several inherent drawbacks of conventional bridges. It is shown that this conventional type of integral bridge still has the following problems: (1) large residual settlements in the backfill, developing a bump immediately behind the abutments, and the development of high residual earth pressure on the back of the abutments by seasonal thermal expansion and contraction of the girder, as well as by traffic loads on the backfill; and (2) large detrimental deformation of the backfill by seismic loads. To alleviate these problems, it is proposed to reinforce the backfill with geosynthetic reinforcement that is firmly connected to the full-height rigid facings (i.e. abutments). A newly proposed integral bridge, called the GRS integral bridge, is constructed in stages: first, geosynthetic-reinforced backfill; second, pile foundations (if necessary); third, full-height rigid (FHR) facings (i.e. abutments); and finally a continuous girder integrated to the top of the two abutments, without using shoes. A series of static cyclic loading tests, laterally on the facing and vertically on the crest of the backfill, and shaking-table tests were performed on models of the conventional and new types of integral bridge, as well as two conventional bridge types comprising RC gravity-type abutments and geosynthetic-reinforced soil-retaining walls, both supporting a girder via shoes. The test results showed high static and dynamic performance of the GRS integral bridge, despite its simple structure and construction procedure, and therefore its low construction cost.

**KEYWORDS:** Geosynthetics, Bridge abutments, Geogrid, Integral bridge, Geosynthetic-reinforced soil-retaining wall, Model test, Seismic behaviour, Shaking-table test

**REFERENCE:** Tatsuoka, F., Hirakawa, D., Nojiri, M., Aizawa, H., Nishikiori, H., Soma, R., Tateyama, M. & Watanabe, K. (2009). A new type of integral bridge comprising geosynthetic-reinforced soil walls. *Geosynthetics International*, 16, No. 4, 301–326. [doi: 10.1680/gein.2009.16.4.301]

### 1. INTRODUCTION

A conventional bridge comprises a single simply supported girder supported by a pair of abutments via hinged shoes (allowing only rotation) and movable shoes (or bearings), or multiple simply-supported girders supported by a pair of abutments and a single or multiple pier(s) via shoes. The abutment, which may be a gravity structure (unreinforced concrete or masonry) or a reinforced concrete (RC) structure, has a number of drawbacks, as follows (Figure 1).

- As the abutment is a cantilever structure that retains unreinforced backfill (Figure 2), earth pressure activated on its back induces large internal force, as well as large thrust force and overturning moment at the bottom of the abutment. Therefore the abutment may become massive, while a pile foundation is necessary unless the supporting ground is strong enough. This drawback becomes increasingly serious with an increase in the wall height.
- Although abutments are usually constructed prior to the construction of the backfill, and the abutment is forced to move when the backfill is constructed, only small movement is allowed for the abutment. Therefore, when constructed on relatively soft ground, a large number of piles may become necessary to prevent movements due to earth pressure, as well as settlement and lateral flow in the subsoil caused by the backfill weight. Large negative friction may be activated on the piles. It is not unusual for the piles to become much longer than the wall height when the soft ground is thick.
- The construction and long-term maintenance of girder shoes and connections between separated simply supported girders are generally costly. The

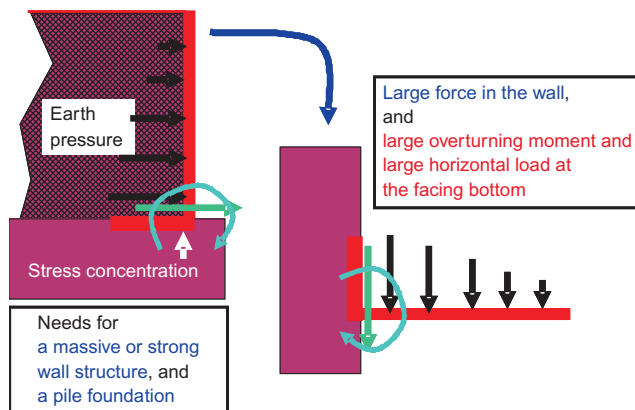


**Figure 2. Inherent problems with conventional retaining walls as a cantilever structure**

girder shoes are a weak part of the whole bridge system when subjected to seismic loads.

- A bump may be formed behind the abutment by long-term settlement of the backfill, owing to its self-weight and traffic loads.
- The seismic stability of the backfill and the abutment supporting the girder via a fixed shoe is relatively low, as experienced in a number of major earthquakes. A large bump may be formed behind the abutment if the backfill deforms largely by seismic loads.

To alleviate these problems, three new bridge systems have been proposed and introduced (Figure 3). The integral bridge (Figures 4a and 4b) has been proposed mainly to alleviate problems with the structural part of the reinforced concrete (RC) and/or steel of the conventional bridge. This new bridge system is now widely used in the UK and North America (in particular, the USA and Canada), mainly it is extremely cost-effective, thanks to

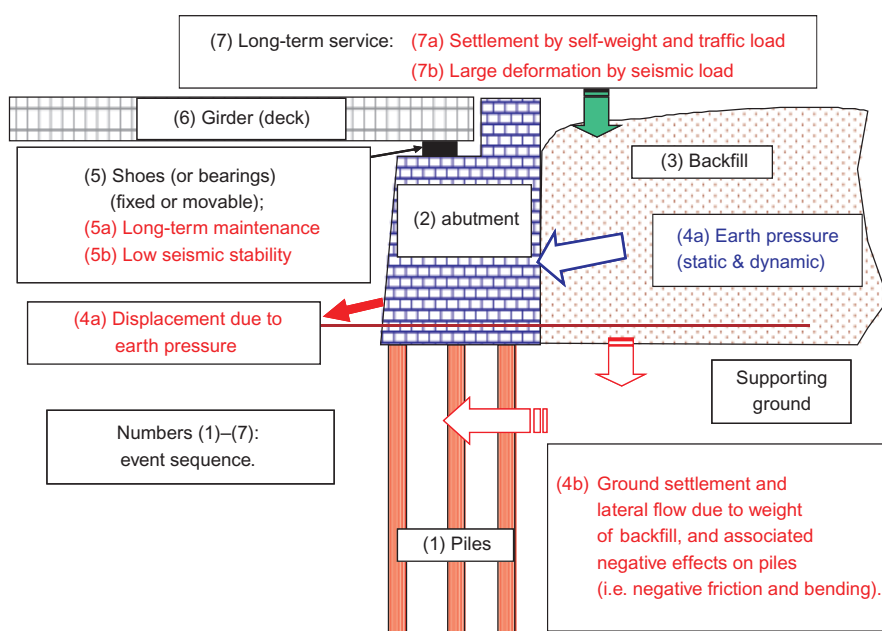


**Figure 1. Technical problems with conventional bridge abutments**

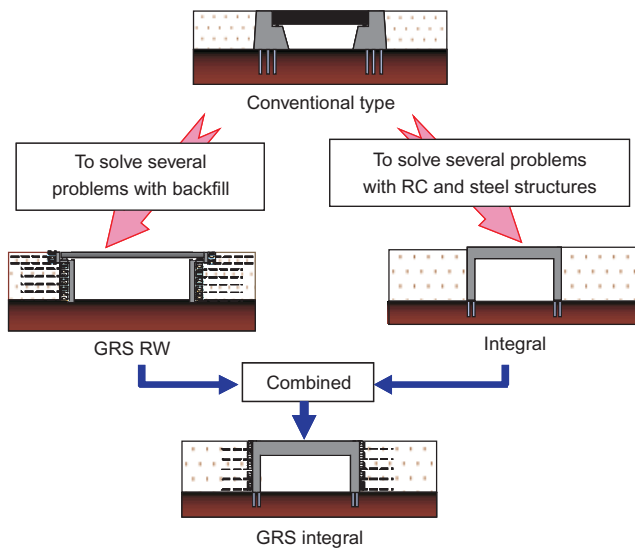


**Figure 3. Development of new bridge types to alleviate technical problems of conventional bridges**

its low construction and maintenance costs, resulting from the non-use of girder shoes (or bearings), and the use of a continuous girder (or deck). Furthermore, the seismic stability of the integrated structural part (i.e. a girder and a pair of abutments) is higher than that of the conventional type (Figure 1), as shown later in this paper. However, this new type of bridge cannot alleviate some of the problems with conventional bridges (Figure 4b). Moreover, a new problem may arise from seasonal thermal expansion and contraction of the girder (Figure 4c), as discussed later in this paper.

Another new type of bridge comprises geosynthetic-reinforced soil (GRS) retaining walls (RWs) with a stage-constructed full-height rigid (FHR) facing as abutments that support a single simply supported girder via shoes and sill beams placed on the reinforced backfill. This new type of bridge, which is herein called the GRS-RW bridge, was developed mainly to alleviate problems with the backfill (Figures 5a and 5b). A number of bridges of this type have been constructed in Japan, because it is more cost-effective than the conventional type (Tatsuoka *et al.* 1997, 2005, 2007a). However, it has the following limitations (Figure 5c).

- When the girder becomes very long, and therefore very heavy, it may exhibit excessive long-term residual settlements due to residual compression of the part of the backfill that is supporting the girder weight. Moreover, large seismic lateral inertia of the girder may be activated on the sill beam that supports the girder via a fixed shoe, even though the seismic stability of the sill beam is generally low (as discussed below and shown later in this paper).
- The construction and maintenance of the girder shoes are costly, as with the conventional type of bridge.
- Although the dynamic stability of GRS-RWs with an FHR facing is very high (e.g. Tatsuoka *et al.* 1998; Koseki *et al.* 2006), the dynamic stability of the sill

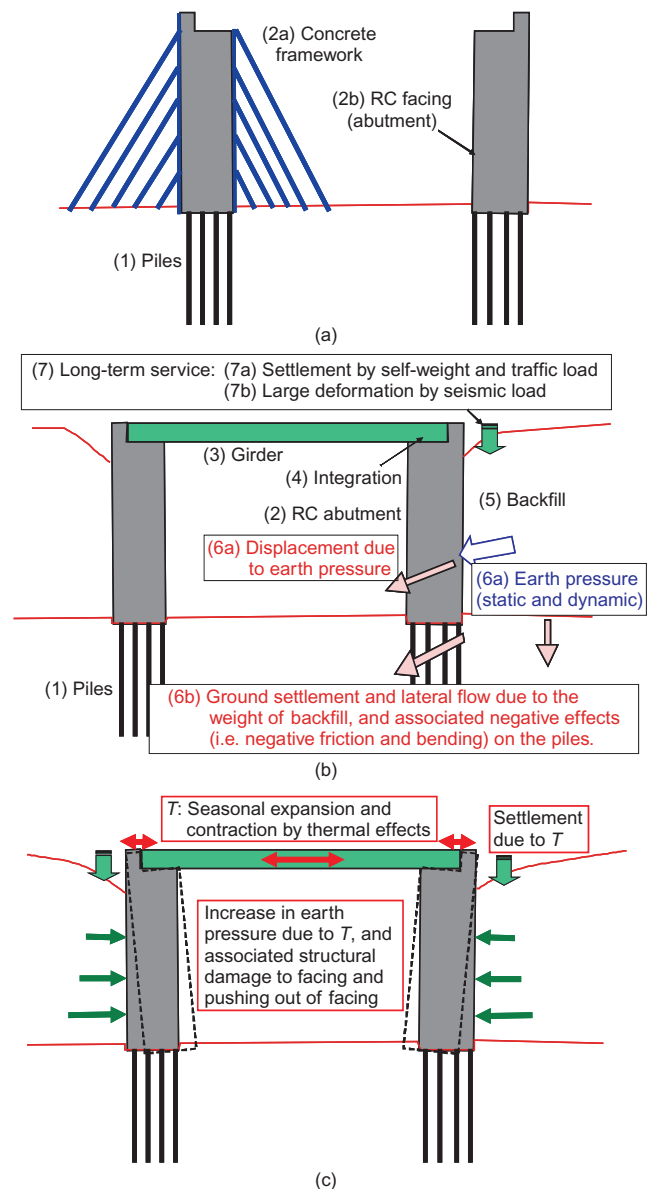


**Figure 4. Integral bridge: (a), (b) construction sequence and associated problems; (c) new problem caused by seasonal thermal expansion and contraction of the girder**

beam supporting the girder via a fixed shoe is not (Aizawa *et al.* 2007; Hirakawa *et al.* 2007b). This is because the mass of the sill beam is very small compared with the girder, and the anchorage capacity of the reinforcement layers connected to its back is small owing to their shallow depths.

A similar bridge type with geosynthetic-reinforced backfill but with facing consisting of modular blocks has been proposed, and several prototypes have been constructed (e.g. Abu-Hejleh *et al.* 2002; Fakharian and Attar 2007). This bridge type has the same drawbacks as above, while not offering the advantages of using stage-constructed full-height rigid facing.

To alleviate the various problems with conventional bridges (Figure 1), as well as these new problems with the integral bridge (Figure 4) and the GRS-RW bridge (Figure 5), the authors have proposed a new bridge type (Figure

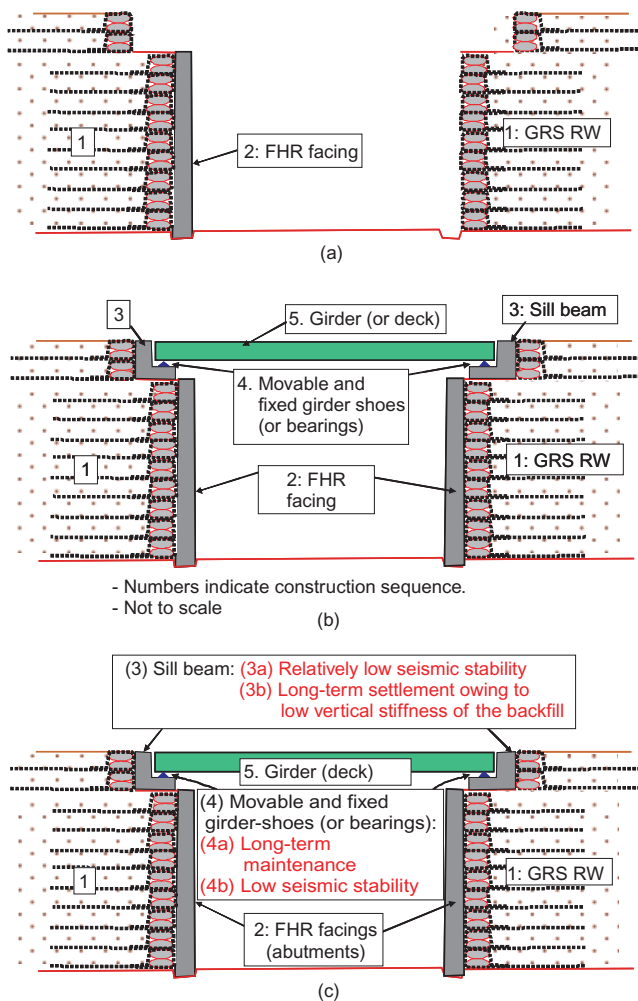


**Figure 5. Bridge comprising GRS-RWs with FHR facing supporting a girder via shoes and a sill beam on reinforced backfill: (a), (b) construction sequence; (c) problems**

6), called the GRS integral bridge (Aizawa *et al.* 2007; Hirakawa *et al.* 2007b; Tatsuoka *et al.* 2007b, 2008a, 2008b). This new type of bridge combines the integral bridge and the GRS-RW bridge, taking advantage of their superior features while alleviating their drawbacks. The objective of this study is therefore to evaluate the structural features and performance of the four types of bridge illustrated in Figure 3 (i.e. conventional, integral, GRS-RW and GRS Integral) by performing static cyclic loading and shaking-table tests on small-scale models.

## 2. INTEGRAL BRIDGE

### 2.1. General

With this type of bridge (Figure 4), as the backfill is not reinforced and therefore is not firmly united with the structural part (i.e. the integrated girder and abutments), the backfill and the structural part do not help each other effectively under static and seismic loading conditions. Therefore their static and seismic stability cannot become very high, as shown below. Moreover, as the girder is integrated with the abutments without using shoes, seasonal thermal expansion and contraction of the girder results

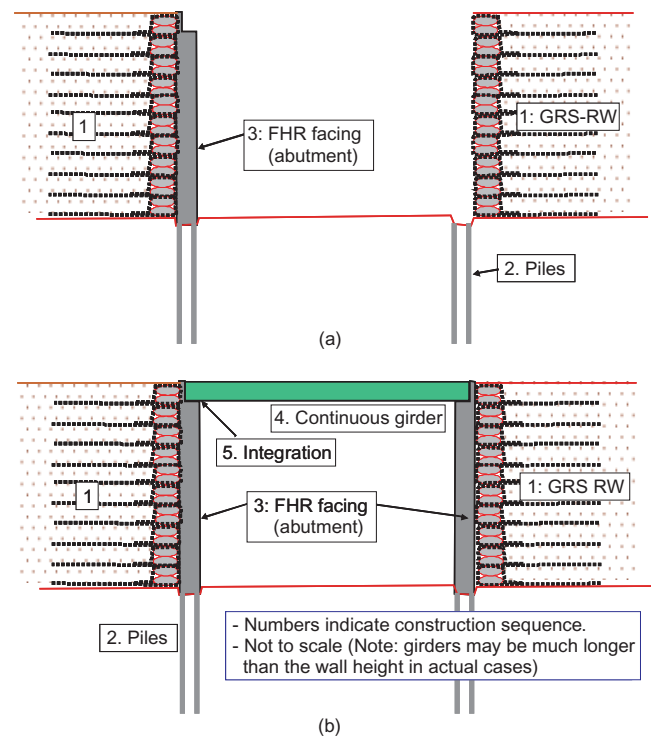


**Figure 6. Construction sequence of GRS integral bridge (with reinforcement connected to facing)**

into lateral cyclic displacements of the abutments (Figure 4c). This may cause two major detrimental effects: (1) the development of high earth pressure on the back of the abutment (i.e. the facing); and (2) large settlements in the backfill, as shown below. The effects of daily thermal deformation of the girder are negligible (England *et al.* 2000; Hirakawa *et al.* 2006, 2007a).

### 2.2. Lateral cyclic loading tests

#### 2.2.1. Test method

A series of model tests were performed under plane-strain conditions to evaluate the effects of lateral cyclic displacements of the facing on the performance of the backfill. The results when the backfill is not reinforced are presented in this section, and those when the backfill is reinforced with geogrid layers (Figure 7b) are explained later in relation to the GRS integral bridge (Figure 6). Figure 7a shows the sand box in which model retaining walls (i.e. facings) were constructed. The backfill was air-dried, poorly graded sub-angular sand, Toyoura sand ( $D_r = 90\%$ ). The unreinforced backfill was produced by air pluviation. Figure 8 shows test cases performed in the present study. The tests with unreinforced backfill (stated NR) are explained herein. The following two conditions at the facing bottom were employed.

- Condition H: The footing bottom is hinge-supported, allowing only rotation, to simulate an FHR facing firmly supported with a pile foundation.
- Condition F: The footing bottom is placed in the subsoil at a depth of only 3.0 cm, allowing fairly free rotation and translation, to simulate an FHR facing not supported with a pile foundation.

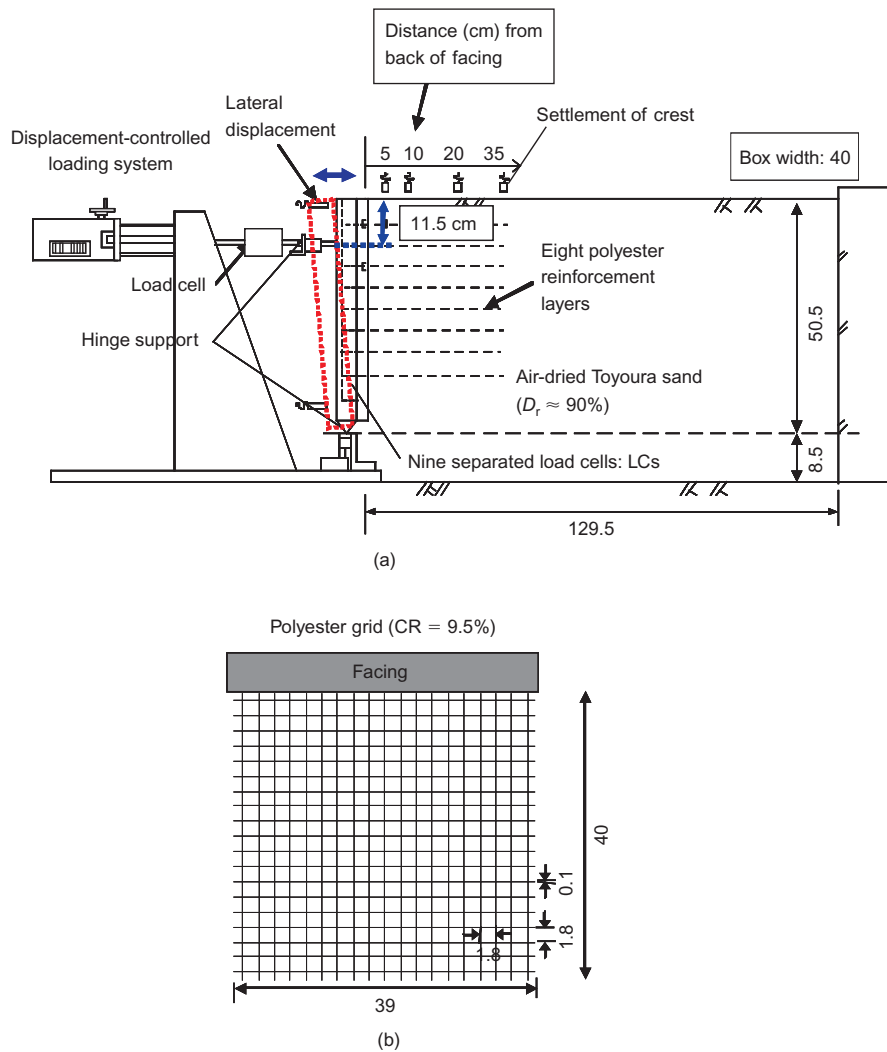


Figure 7. (a) Static model tests to evaluate negative effects of lateral cyclic displacements at top of facing (test conditions R&C and H-A, Figure 8); (b) model reinforcement (Nojiri *et al.* 2006; Hirakawa *et al.* 2007b) (all dimensions in cm)

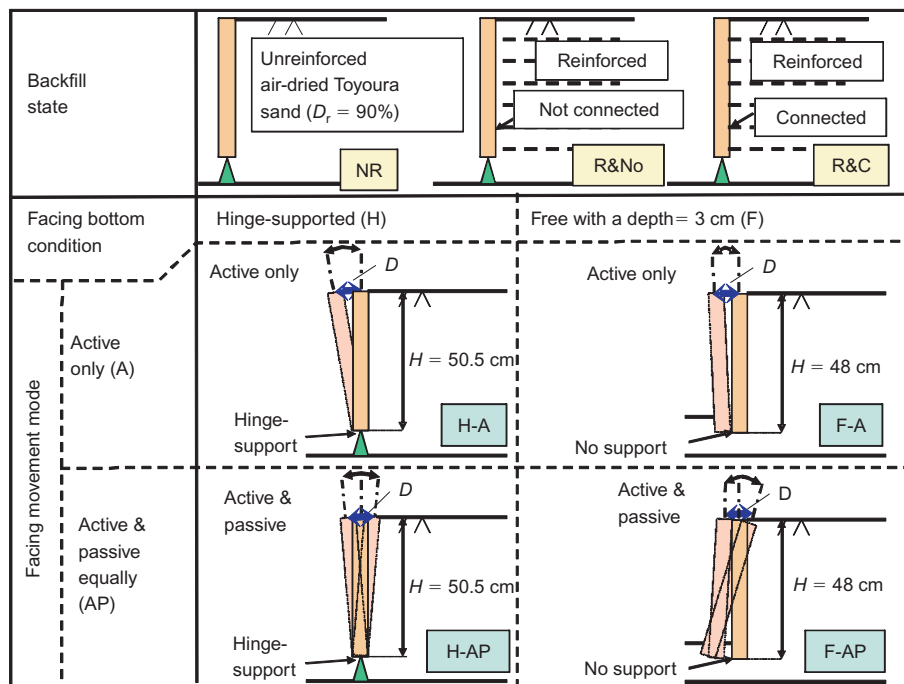


Figure 8. Lateral cyclic loading test cases

The wall height,  $H$ , is equal to 50.5 cm in condition H, and 48 cm in condition F. At a distance of 11.5 cm down from the facing top, the FHR facing was cyclically displaced at a displacement rate of 0.004 mm/s (converted to the value at the facing top). The following two cyclic displacement modes were employed.

- Mode A: The facing top was displaced between the neutral state (i.e. when the displacement at the facing top,  $d$ , is equal to zero) and an active state with a fixed amplitude ( $D$ ).  $d$  is defined as positive in the active state.
- Mode AP: The facing top was cyclically displaced first towards the active state and between  $d = D/2$  (active state) and  $-D/2$  (passive state).

Modes A and AP simulate the behaviours of the abutment of integral bridges that are completed in summer and fall, respectively.

### 2.2.2. Test results

In the following, first, the results for mode A are reported. Figure 9 shows a typical test result when the backfill is unreinforced (NR); the facing bottom is hinged (H); and  $D/H = 0.6\%$  in the active displacement mode (A). Figure 9 shows the time histories of: (b) the lateral displacement at the facing top,  $d$ ; (c) the backfill settlement at different distances,  $L$ , from the back of the facing; and (d) the total earth pressure coefficient,  $K = 2Q/H^2\gamma$ , where  $Q$  is the total earth pressure per width of the facing measured with nine local two-component load cells (measuring normal and shear loads),  $H$  is the wall height (50.5 cm), and  $\gamma$  is the dry unit weight of the backfill (1.60 gf/cm<sup>3</sup>). The following trends of behaviour may be seen.

- By a small amplitude of lateral cyclic displacement of the facing top equal to  $D/H = 0.6\%$ , the peak value of earth pressure in the respective cycles increases significantly with cyclic loading. After five cycles (i.e. after five years in the prototype), the  $K$  value becomes higher than about 3.
- Corresponding to the above, the backfill settles down significantly, and by more at places closer to the facing. At  $L/H = 5 \text{ cm}/50.5 \text{ cm} \sim 0.1$ , the settlement,  $S_g$ , after five cycles exceeds 1% of the wall height,  $H$ . The settlement still increases significantly with further cyclic loading.

These two trends are explained later by the dual ratchet mechanism in the backfill (England *et al.* 2000; Tatsuoka *et al.* 2008a, 2008b). When these trends of behaviour take place with full-scale integral bridges (with unreinforced backfill), this earth pressure increase may cause structural damage to the facing structure, the facing bottom may be severely pushed out, and a large bump may develop behind the facing. An approach slab is often used to alleviate the problem of a bump. However, this method cannot alleviate the other problems illustrated in Figure 1.

Figure 10 shows the relationships between the earth pressure coefficient,  $K = 2Q/H^2\gamma$ , and the normalised facing displacement,  $d/H$ , from two typical tests on unreinforced backfill (NR) in which the facing displacement is either active only (A) or equally active and passive (AP), with the footing bottom being hinge-supported (H).  $D/H$  is equal to 0.2%. Figure 11a shows the relationship between the peak earth pressure coefficient,  $K_{\text{peak}}$ , in the respective cycles and the number of loading cycles,  $N$ , including the data presented in Figures 9 and 10. The test results when the backfill is reinforced shown in this figure are discussed

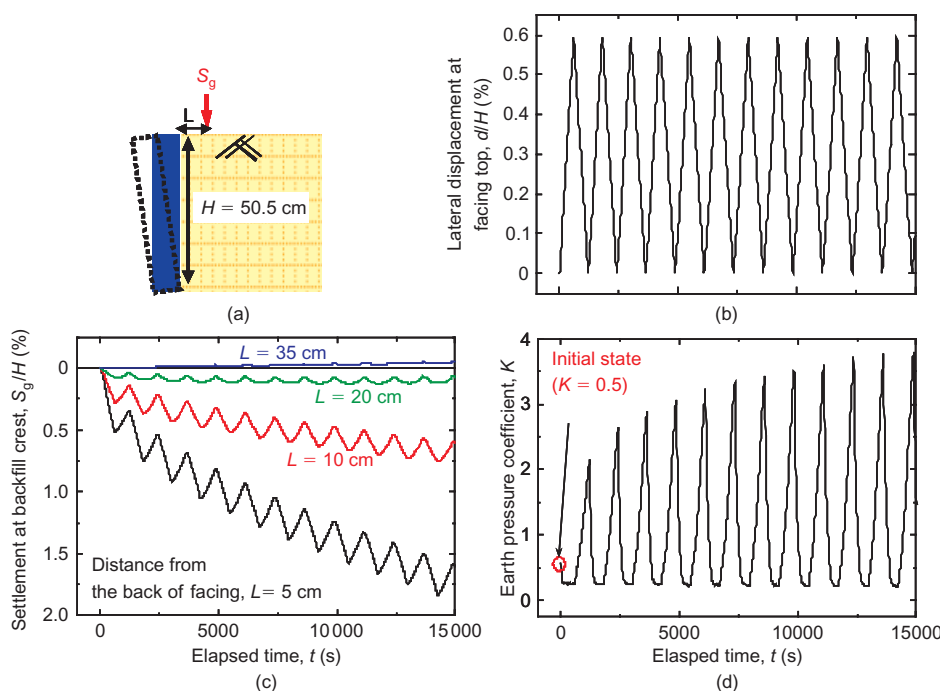


Figure 9. (a) Test method. Typical test results; time histories of: (a) horizontal movement at top of facing; (c) backfill settlement; (d) total earth pressure, unreinforced Toyoura sand (cases NR and H-A)

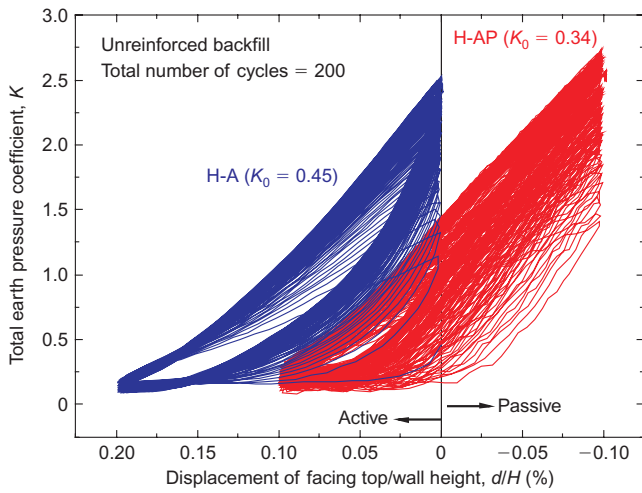


Figure 10. Relationship between total earth pressure coefficient,  $K$ , and horizontal displacement at the facing top,  $d/H$ , for unreinforced backfill and hinge-supported facing bottom (cases NR and H-A/H-AP)

with cyclic loading becomes stronger with an increase in the facing displacement. Figure 12a summarises the values of  $K_{peak}$  at selected numbers of loading cycles,  $N$ , plotted against  $D/H$  when the backfill is unreinforced (NR), the facing displacement is active only (A), and the facing bottom is hinge-supported (H). The earth pressure at a given number of cycles increases rather linearly with an

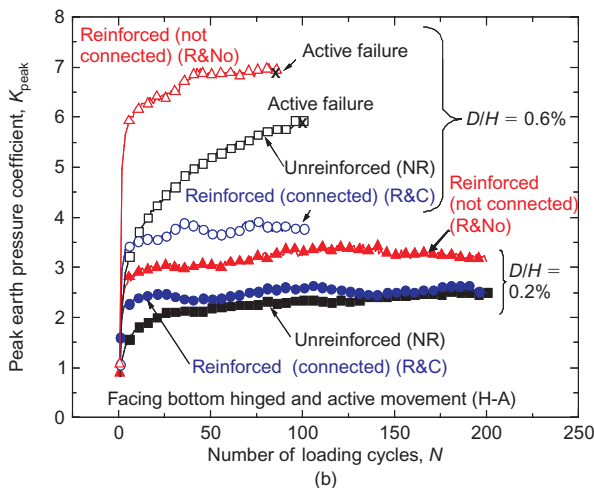
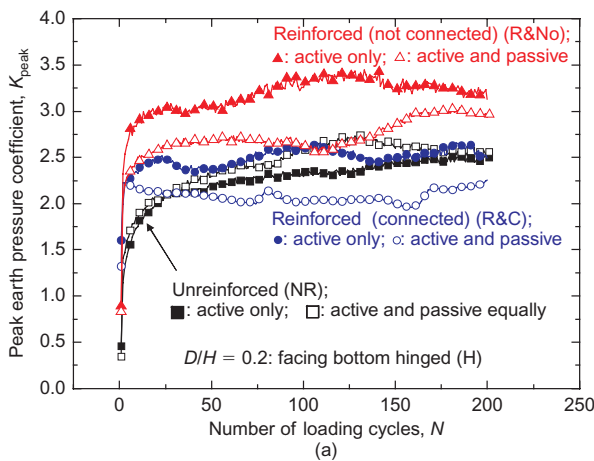
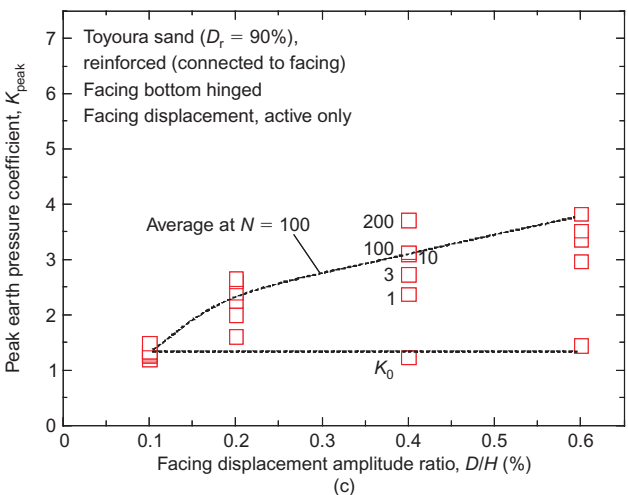
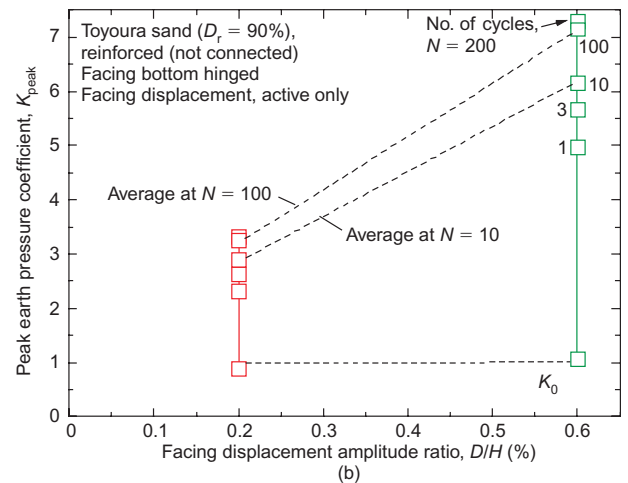
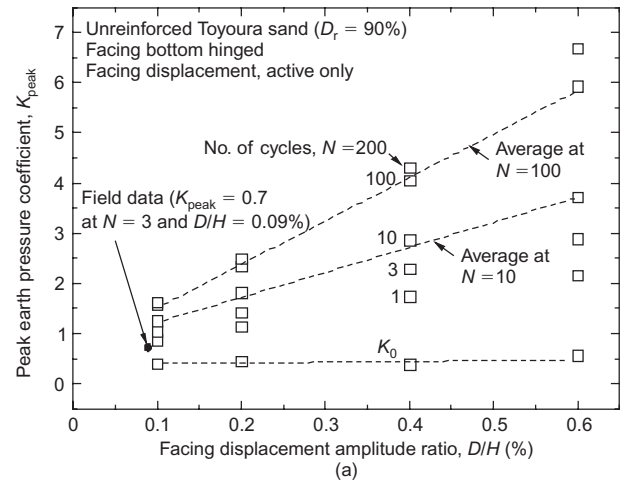


Figure 11. Relationships between  $K_{peak}$  and number of loading cycles,  $N$ , for hinged footing bottom (H): (a)  $D/H = 0.2\%$  (cases H-A & H-AP); (b)  $D/H = 0.2\%$  and  $0.6\%$  (case H-A)

later. Figure 11b compares the behaviours when  $D/H$  is equal to  $0.2\%$  and  $0.6\%$  when the facing displacement is active only (A). It may be seen that the trend for the peak earth pressure coefficient,  $K$ , to increase at a very high rate

Figure 12. Peak earth pressure coefficients (case NR and H-A, Figure 8): (a) unreinforced backfill; (b) backfill reinforced without connection to facing; (c) backfill reinforced with connection to facing

increase in  $D/H$ . These test results are consistent with previous laboratory model tests (Ng et al. 1998; England et al. 2000), as well as with the full-scale field behaviour for three years (i.e.  $N = 3$ ; Hirakawa et al. 2006).

The other major detrimental effect of lateral cyclic displacement of the facing is gradual but eventual large settlements in the unreinforced backfill (Figure 9c), associated with the development of an active wedge in the backfill, as typically seen in Figure 13. Figure 14a shows the relationship between the backfill settlement at the neutral state (i.e.  $d = 0$ ) at 5 cm from the back of the facing and the number of loading cycles,  $N$ , when  $D/H = 0.2\%$  and the facing displacement is either only active (A) or equally active and passive (AP). The backfill is either unreinforced or reinforced (with and without the connection of reinforcement to the facing). Figure 14b compares the backfill settlement when  $D/H = 0.2\%$  and  $0.6\%$  when the facing displacement is only active (A). The results when the backfill was reinforced are discussed later. The settlement of the unreinforced backfill increases with an increase in the facing displacement amplitude ( $D/H$ ). Moreover, the backfill settlement for the same  $D/H$  is larger when the facing displacement is only active (A) than when it is equally active and passive (AP). This is because an active wedge can be formed more easily when the facing moves only on the active side (Figure 13).

### 2.2.3. Dual ratchet mechanism

High passive earth pressures and large settlements in the backfill associated with the formation of an active wedge by lateral cyclic displacement of the facing with small amplitude, as described above, are due to the dual ratchet mechanism in the backfill, illustrated in Figure 15 and explained below. Figure 16 shows the time histories of lateral displacement at the facing top and the backfill settlement ( $L = 5$  cm) presented in Figure 9 that are interpreted by this mechanism.



**Figure 13.** Typical active failure in unreinforced backfill developed by lateral cyclic displacement of facing;  $D/H = 0.2\%$  (active only)

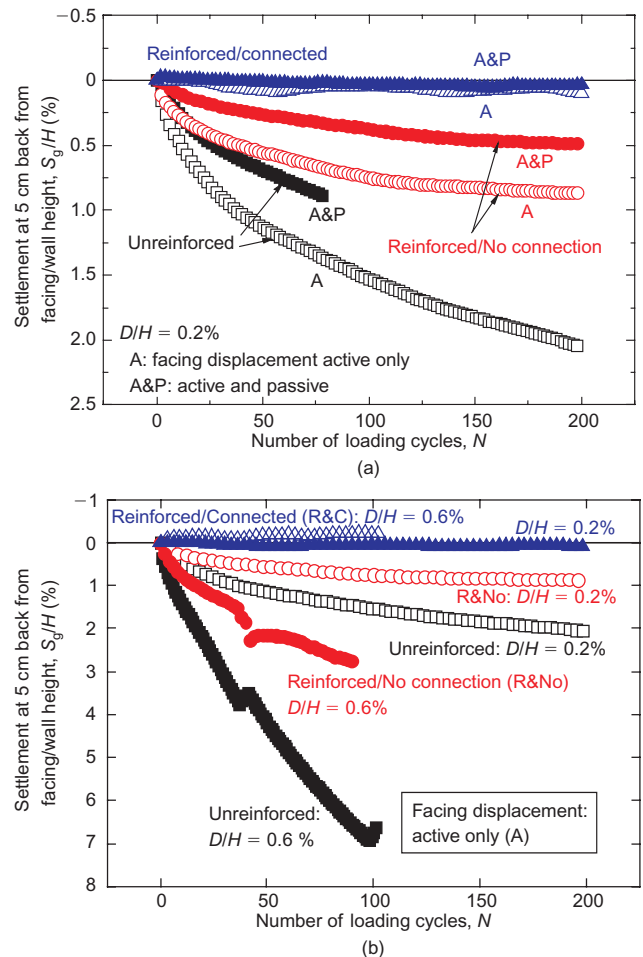


**Figure 14.** Residual settlement (when  $d = 0$ ) at 5 cm from facing in unreinforced and reinforced backfill plotted against number of loading cycles: (a)  $D/H = 0.2\%$  (cases A-H and AP-H); (b)  $D/H = 0.2\%$  and  $0.6\%$  (case A-H)

- (1) Suppose that a small active displacement of the facing takes place, and small active sliding develops, forming an active wedge (i.e. process  $S \rightarrow A1$  in Figures 15 and 16).
- (2) Subsequently, the facing is subjected to small passive displacement (i.e. process  $A1 \rightarrow P1$ ). In this process the active sliding is not reactivated, but a passive wedge zone that is much larger than the active wedge develops, while the active wedge deforms as part of the passive zone.
- (3) When the second small active displacement of the facing occurs, the active sliding develops further (i.e. process  $P1 \rightarrow A2$ ), while the part outside the active wedge does not deform.
- (4) When the facing is subjected to the second small passive displacement (i.e. process  $A2 \rightarrow P2$ ), again, the active sliding is not reactivated, while the passive deformation develops further.

Processes (1)–(4) are repeated in the course of lateral cyclic displacement of the facing. Although the active sliding is small in each cycle, it accumulates with cyclic loading, as illustrated in Figure 16a (i.e. the active ratchet mechanism), which eventually results in active failure, as

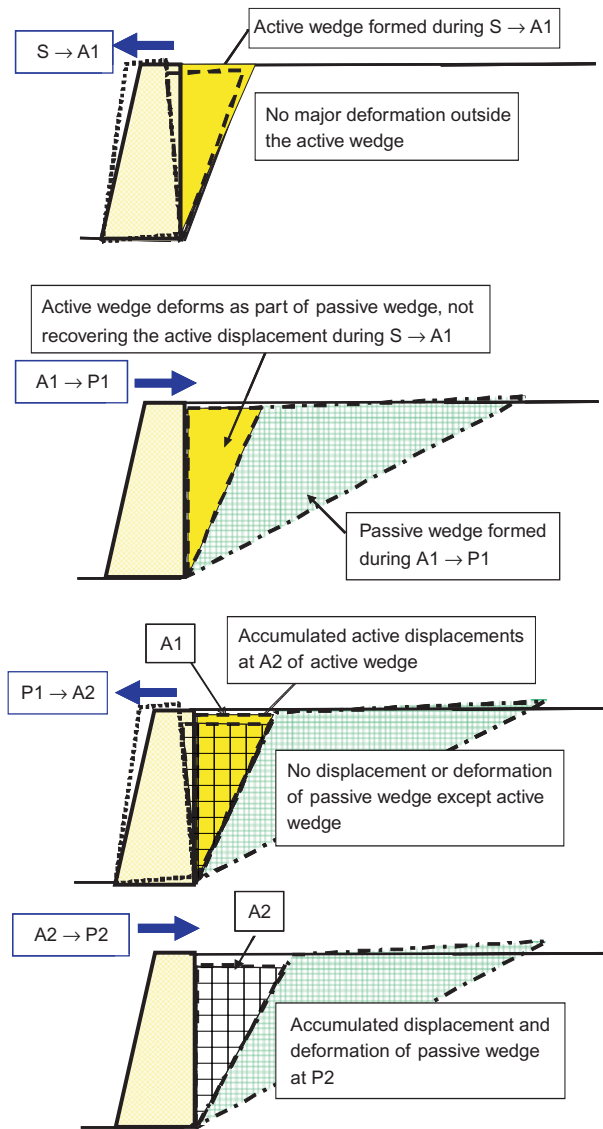


Figure 15. Dual ratchet mechanism when the facing bottom is hinge-supported

the one that takes place during monotonic active loading, as shown in Figure 17. Although it is also small in each cycle, the passive strain in the passive zone accumulates with cyclic loading (Figure 16a), which gradually increases the passive earth pressure with cyclic loading (i.e. the passive ratchet mechanism). As the passive displacement of the facing when the passive failure takes place during monotonic passive loading is very large (Figure 17), the active failure occurs long before the passive failure during cyclic loading. At the crest of the backfill, large settlement takes place associated with the accumulation of active sliding with cyclic loading, while heaving takes place by cumulative passive deformation of the passive zone (Figure 16b). The actual settlement that occurs in the backfill is a summation of those due to the dual ratchet mechanism explained above and those caused by cumulative compressive volumetric strains in the backfill that occur by cyclic straining.

There are two other mechanisms that increase the earth pressure with cyclic loading, although they are less important than the dual ratchet mechanism. The first is an

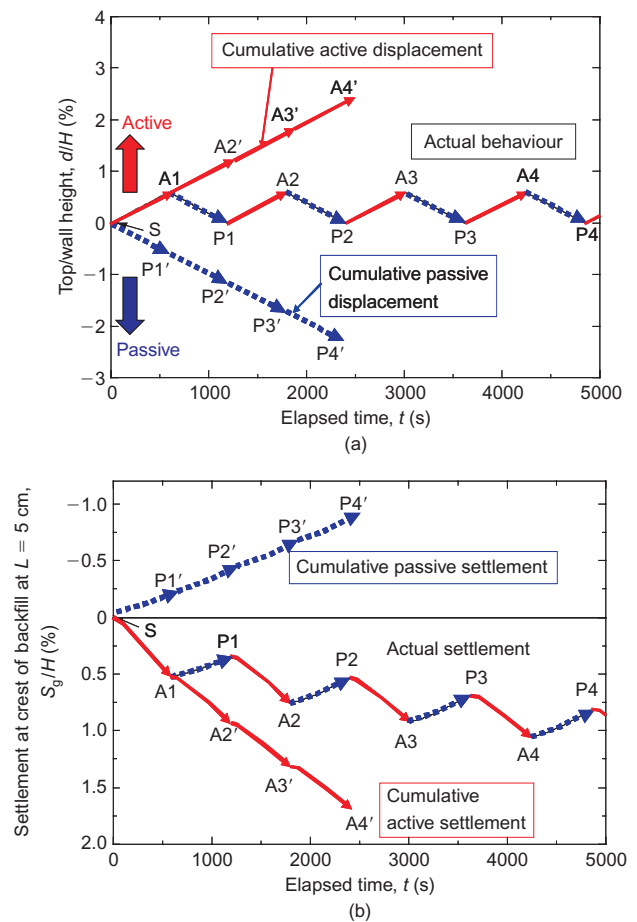


Figure 16. Interpretation by the dual ratchet mechanism of: (a) lateral displacement at the facing top; (b) backfill settlement

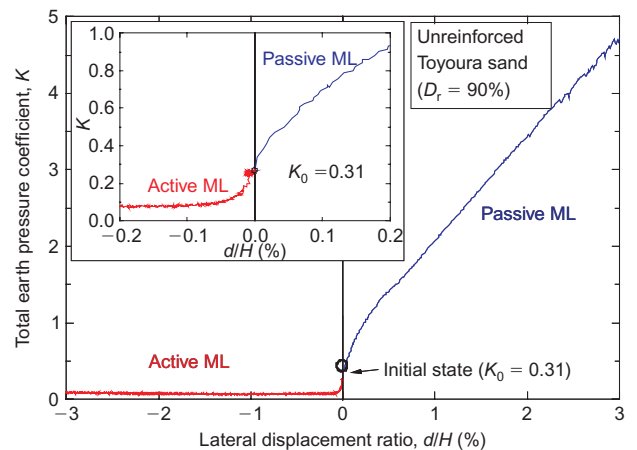


Figure 17. Earth pressure during active and passive monotonic loading on unreinforced backfill; the facing bottom is hinged

increase due to cyclic strain-hardening effects (Tatsuoka *et al.* 2003), by which the peak-to-peak secant modulus of the hysteresis stress–strain loop for fixed strain amplitude increases with cyclic loading. The second is an increase in the active earth pressure with an increase in the active displacement of the facing after it exhibits the minimum caused by strain-softening in the shear band, as seen from

Figure 17. A gradual increase in the smallest earth pressure at the active state in each cycle with cyclic loading seen in Figure 10 is due to this mechanism.

The dual ratchet mechanism also becomes active if relative lateral displacements take place repeatedly between the facing and the backfill during a seismic event. This is typically the case with integral bridges subjected to seismic loadings, where the relative distance between a pair of abutments does not change during seismic loading. Also in this case, large backfill settlement may take place in the backfill, while the earth pressure on the back of the facing may increase significantly.

It may be seen from the above that integral bridges without reinforcement of the backfill cannot be free from two detrimental effects (large active deformation of the backfill and large passive earth pressure) due to thermal deformation of the girder and the seismic response of the bridge. It is shown later that these drawbacks with integral bridges can be effectively alleviated by reinforcing the backfill with geosynthetic reinforcement layers connected to the back of the facing.

2.2.4. Effects of facing bottom conditions

When the facing bottom is not supported by a pile foundation and is therefore fairly free for lateral sliding and rotation, it can easily be pushed out. Therefore, when the unreinforced backfill is subjected to lateral cyclic loading at the facing caused by seasonal thermal compression and expansion of the girder, if the facing bottom is not firmly supported by a pile foundation, active failure takes place more easily (Figure 18a) and the settlement increases significantly (Figure 18b), associated with a significant decrease in the earth pressure (Figure 19).

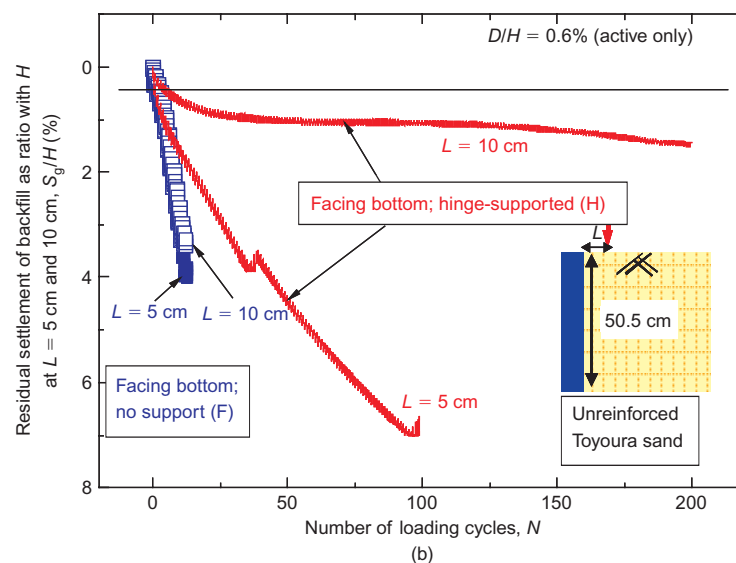
3. GRS-RW BRIDGE: IMPROVING THE PERFORMANCE OF BACKFILL

3.1. Several geotechnical proposals

Several geotechnical solutions have been proposed to improve the seismic performance of the backfill behind the abutment (Figure 20; Tatsuoka 2004; Tatsuoka et al.



(a)



(b)

Figure 18. Effects of footing bottom condition on behaviour of unreinforced backfill,  $D/H = 0.6\%$  and active only: (a) failure mode; (b) backfill settlement

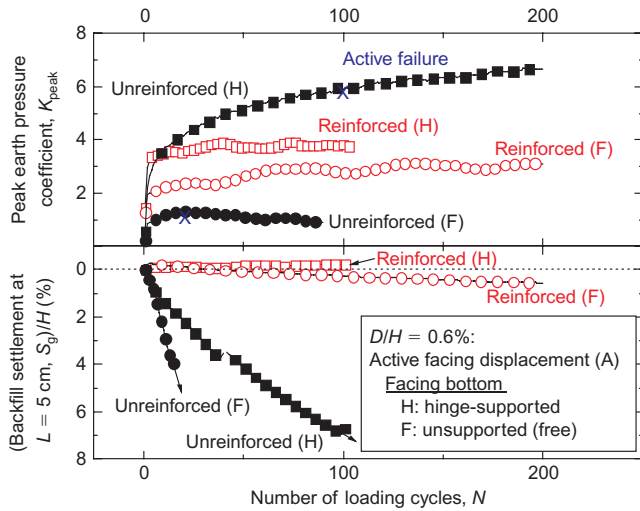


Figure 19. Effects of backfill reinforcement and facing bottom conditions

2005). Japanese railway engineers constructed a trapezoidal zone of well-compacted, well-graded gravelly soil behind a conventional bridge abutment (type a1 in Figure 20). However, its performance during several previous earthquakes in Japan was very poor. Watanabe *et al.* (2002) and Tatsuoka *et al.* (2005) confirmed the above by performing model shaking-table tests. They also showed that the seismic stability of a similar type comprising a trapezoidal zone of cement-mixed gravel (type a2, Figure 20) is not sufficiently high. Therefore the other types shown in Figure 20 have been tested, as described below.

### 3.2. Geosynthetic-reinforced soil-retaining walls with a stage-constructed FHR facing

#### 3.2.1. General

Figure 21 illustrates the staged construction procedure for a geosynthetic-reinforced soil retaining wall (GRS-RW) with a full-height rigid (FHR) facing. This new type is now one of the standard retaining wall construction technologies in Japan, and the total wall length of permanent retaining walls is more than 100 km at more than 700 sites as of June 2008.

This new GRS-RW has several advantageous features, as described below. The first is the staged construction of an FHR facing, consisting of the following steps.

- (1) A small foundation (i.e. a levelling pad) is constructed for the facing.
- (2) A full-height GRS-RW with wrapped-around wall face is constructed by placing gravel-filled bags at the shoulder of each soil layer to help achieve better compaction of the backfill close to the wall face. Gravel-filled bags stacked at the wall face function as a temporary facing until the next step.
- (3) After the major part of the ultimate deformation of the backfill and the subsoil layer beneath the wall has taken place, a thin concrete facing (i.e. 30 cm or more in thickness), lightly reinforced with steel (i.e. an FHR facing), is constructed by casting-in-place fresh concrete. A firm connection between the FHR facing and the main body of the wall can be ensured by placing fresh concrete directly on the geogrid-

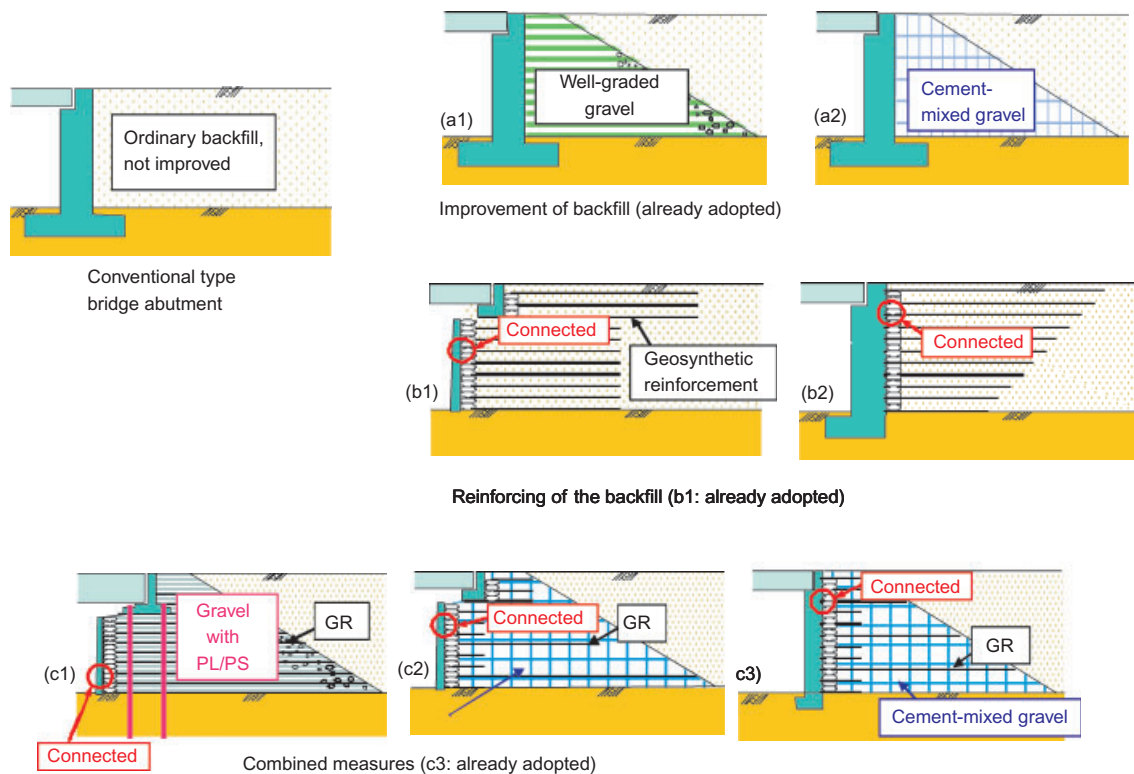


Figure 20. Different geotechnical proposals to improve the performance of abutments

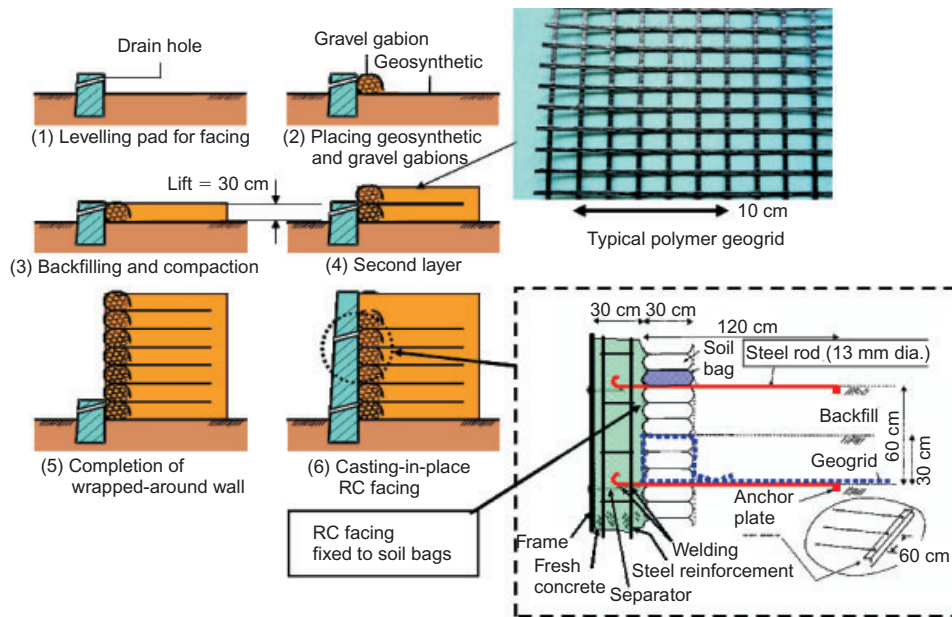


Figure 21. Staged construction of GRS-RW with FHR facing (Tatsuoka et al. 1998, 2007a)

covered wall face, allowing the concrete to enter the apertures of the wrap-around geogrid.

If an FHR facing is erected and propped before the start of construction of the backfill, the connection between the reinforcement and the facing may be damaged by differential settlement between the facing and the backfill, caused by deformation of the backfill and supporting ground. Moreover, sufficient tensile force is mobilised in the geosynthetic reinforcement only after the propping is removed after the wall is constructed, which may result in uncontrolled and relatively large lateral outward displacements of the facing that may last for a long time after the wall is opened to service. The staged construction procedure can alleviate these two problems.

The second advantageous feature is the firm connection of the reinforcement layers to the FHR facing, as a result of the staged construction described above. The importance of this factor for wall stability is illustrated in Figures 22 and 23 (Tatsuoka 1992). This factor is particularly important in ensuring high seismic stability

(Tatsuoka et al. 1998; Koseki et al. 2006). A conventional retaining wall is basically a cantilever structure that resists the active earth pressure from the unreinforced backfill by the moment and the thrust force activated at its base (Figure 2). Relatively large earth pressure, similar to the active earth pressure activated on a conventional retaining wall, may be activated on the back of the FHR facing of GRS-RW because of the high connection strength between the reinforcement and the facing. However, this high earth pressure results in a high confining pressure in the backfill, and therefore high stiffness and strength of the backfill, which results in better performance than in the case without a firm connection between reinforcement and facing (Figure 23). That is, a substantial reduction of earth pressure is *not* the objective of this new retaining wall technology. As the FHR facing behaves as a continuous beam supported at a large number of levels with a small span, typically 30 cm (Figure 22), only a small force is activated inside the FHR facing, which results in a much simpler facing structure. At the same time, the overturning moment and lateral thrust force activated at the bottom of the facing become small, which makes the use of a pile foundation unnecessary unless the supporting

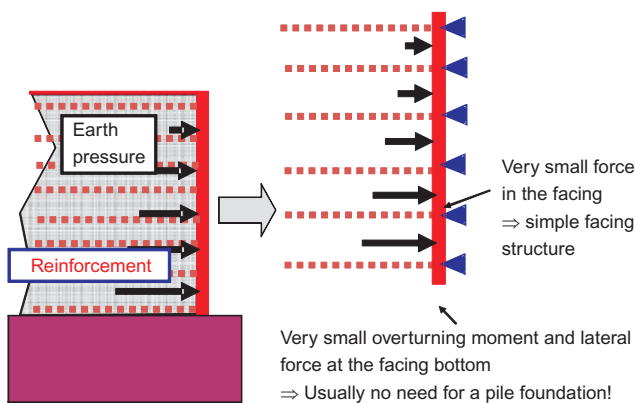


Figure 22. FHR facing as a continuous beam supported at many places with a small span

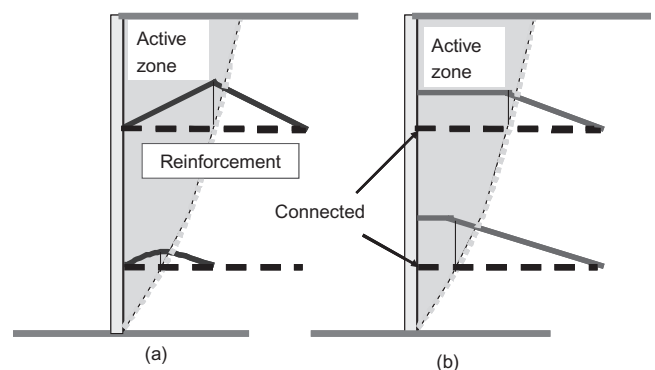


Figure 23. Tensile force distribution in the reinforcement: (a) no connection; (b) firm connection

ground is very soft and weak. Moreover, with an FHR facing, a GRS-RW can support concentrated loads, vertical and/or horizontal, that are applied to at, or immediately behind, the facing. When concentrated load is applied to the top of the facing, all the geosynthetic layers connected to the facing for the full wall height can contribute to the stability of the facing. When the concentrated load is applied to the backfill immediately behind the facing, an FHR facing prevents the occurrence of local failure only in the backfill zone close to the location where the concentrated load is applied, while not allowing failure planes to pass through intermediate heights along the wall face. An increase in the static and dynamic stability of a GRS-RW by using an FHR facing has been reported by several researchers (e.g. Tatsuoka 1992; Murata *et al.* 1994; El-Emam and Bathurst 2005; Huang and Wu 2007). The GRS integral bridge takes advantage of these features, as described later.

The third advantageous feature is the use of planar polymer geogrid reinforcement for cohesionless backfill to ensure good interlocking with the backfill. Thus the anchorage length of geosynthetic reinforcement that is necessary to resist tensile load equivalent to the tensile rupture strength of the reinforcement becomes relatively short, unlike metal strip reinforcement. The GRS integral bridge, explained later, takes advantage of this feature.

Figure 24 shows a typical GRS-RW with an FHR facing that was constructed during 1995–2000 to support one of the busiest urban rapid transits, the Yamanote line. Numerous case histories have shown that this type of GRS-RW is much more cost-effective than conventional retaining walls. The construction cost is much lower, the construction speed is much higher, and much lighter construction machinery can be used, which also results in greatly reduced CO<sub>2</sub> emissions. It is also important that the performance of this new type RWs is equivalent to, or even better than, that of conventional soil retaining walls.

Taking advantages of the described above, several bridges comprising a pair of GRS-RWs with an FHR facing supporting a simply supported girder (type b1 in Figure 20; Tatsuoka *et al.* 1997, 2005) have been constructed. Although this GRS-RW bridge (Figure 5) is structurally simpler and more cost-effective than the conventional bridge (Figure 1), it has the three major limitations that were discussed earlier in relation to Figure 5c: direct girder support of the backfill, the use of shoes, and a relatively low stability of the sill beams. Type b2 (Figure 20), in which a girder is placed on top of the FHR facing via a shoe, is dynamically more stable than type b1 (Watanabe *et al.* 2002; Tatsuoka *et al.* 2005). However, the problem of using shoes remains.

## 4. GRS INTEGRAL BRIDGE

### 4.1. Several forerunners

To alleviate the problems with abutment type b1 (Figure 20) of the GRS bridge, it is very effective to preload the reinforced backfill vertically and then maintain a relevant amount of vertical prestress, typically about half of the

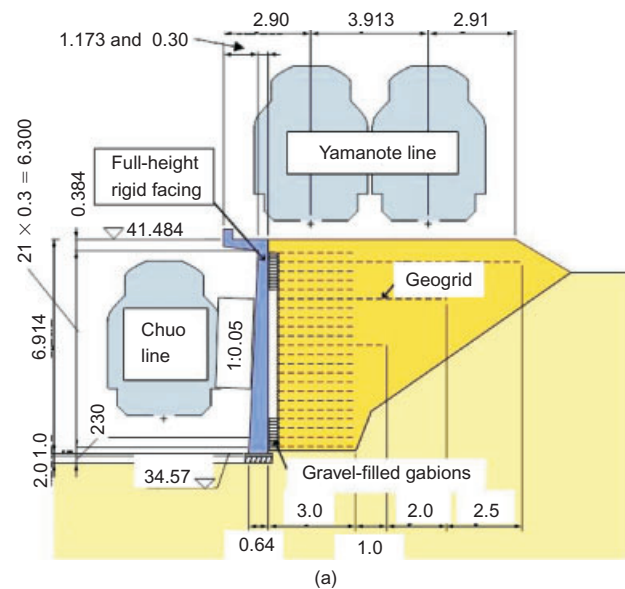


**Figure 24. GRS-RW supporting a rapid transit, near Shinjuku station in Tokyo (Yamanote line): (a) typical cross-section (all dimensions in m); (b) under construction (1995–2000); (c) completed wall**

preload, in the backfill during long-term service (i.e. PL and PS technology: type c1 in Figure 20). This was validated by laboratory model tests (Shinoda *et al.* 2003a) and by the long-term performance of a prototype railway bridge pier (Uchimura *et al.* 2003a, 2005). Moreover, Uchimura *et al.* (2003b) and Tatsuoka *et al.* (2005) showed that the seismic stability of a PL-PS reinforced bridge pier and abutment is very high. The results of

laboratory model shaking-table tests (Shinoda *et al.* 2003b; Nakarai *et al.* 2002) showed that this is particularly the case if high prestress can be maintained during dynamic loading by using a ratchet mechanism to fix the ends of tie rods. However, no prototype bridge of type c1 has been constructed, because the possible long-term maintenance works of the ratchet system are not preferred by practising engineers.

Abutment types c2 and c3 (Figure 20) were then proposed, which combine, respectively, types b1 and b2 with type a2. Type c3 was adopted by Japanese railway engineers, and the first prototype was constructed for a new bullet train line in Kyushu (Figure 25). Type c3 abutments are constructed by the staged procedure (Figure 21), and a bridge girder is finally placed on the top of the RC facing via a fixed shoe (Figure 25a). The conventional RC abutment (Figure 1) laterally supports the unreinforced backfill, which may activate large static and dynamic earth pressure on the back of the facing. In contrast, the RC abutment (i.e. facing) of type c3, which is supporting the girder, is laterally supported by the reinforced backfill, while the backfill does not activate dynamic active earth pressure on the back of the RC abutment. Despite the advantages described above, bridge abutments of type c3 are not free from problems caused by the use of shoes.

#### 4.2. Combined integral GRS-RW bridge

It was then proposed to modify type c3 bridge abutments by integrating a continuous girder directly to the top of a

pair of facings, without using shoes (Tatsuoka *et al.* 2007b, 2008a, 2008b). It is not necessary to improve the backfill by cement mixing in usual cases. This new bridge type, called the GRS integral bridge (Figure 6), is a combination of the integral bridge and the GRS-RW bridge (Figure 3), and has the following features in structure and construction.

- (1) The backfill is reinforced with geosynthetic reinforcement layers that are firmly connected to the back of FHR facings (i.e. abutments).
- (2) The bridge abutments are constructed by the following staged construction procedure:
  - (a) First, a pair of GRS-RWs, with the wall face wrapped around with geogrid reinforcement (without an FHR facing), are constructed.
  - (b) Pile foundations for the abutments are then constructed, if necessary. If the deformation of the supporting ground by the construction of the backfill is not significant, pile foundations may be constructed before GRS-RWs (without an FHR facing) for better constructability.
  - (c) FHR facings are constructed by casting fresh concrete in place on the wall face.
  - (d) A continuous girder is placed on and integrated to the crest of the RC abutments.

As this staged construction procedure is a modification of that described in Figure 21, it has the same advantages as listed in the previous section. In particular, the pile foundation is much lighter than that used with conventional bridge abutments.

#### 4.3. Model tests

##### 4.3.1. Lateral cyclic loading tests

The significant advantages of reinforcing the backfill with geosynthetic reinforcement layers that are firmly connected to the back of the facing when the facing is subjected to lateral cyclic displacements due to seasonal thermal expansion and contraction of a girder were confirmed by a series of lateral cyclic loading tests (Figure 7). In test case R&C (Figure 8), the reinforcement layers were connected to the facing to simulate an abutment of a GRS integral bridge (Figure 6). In test case R&No, the reinforcement layers were not connected to the facing, to evaluate the effects of the connection of the reinforcement to the facing. If a prototype structure of this type is to be constructed, after a pair of RC abutments and a continuous girder are constructed and integrated, the backfill is constructed and reinforced with reinforcement layers that are not connected to the facing. As shown below, the performance of this type of bridge is very low. The backfill was air-dried Toyoura sand ( $D_r = 90\%$ ). Reinforced backfill was constructed by compaction by hand-tamping so that the temporary level sand surface on which the reinforcement layers were placed was more easily prepared, and better interlocking between the backfill and the reinforcement could be ensured than with the air-pluviation method. As can be seen from Figure 26, although the different preparation methods for the unrein-

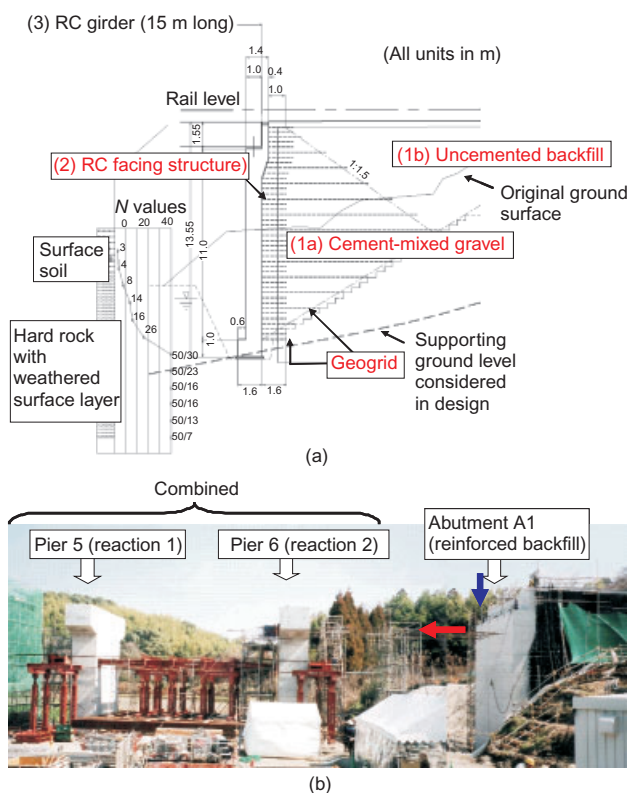


Figure 25. Prototype bridge abutment of type c3 (Figure 20) at Takada, Kyushu, for new bullet train line (Tatsuoka *et al.* 2005): (a) structural details (numbers 1–3 indicate construction sequence); (b) lateral and vertical loading test of facing

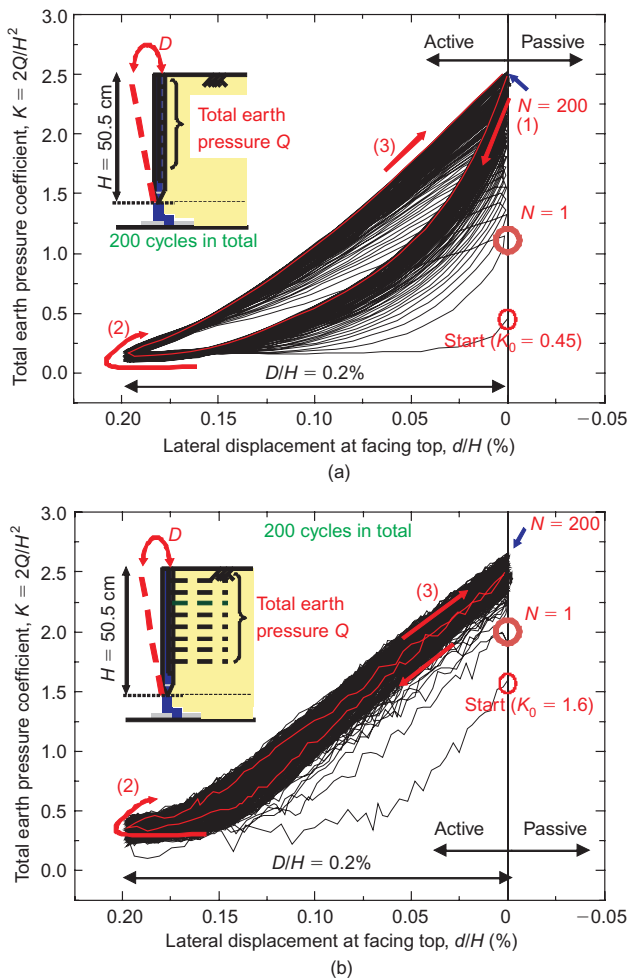


Figure 26. Effect on earth pressure of reinforcing the backfill with reinforcement connected to facing ( $D/H = 0.2\%$ )

forced and reinforced backfill models resulted in different initial earth pressure coefficients, this difference quickly disappeared with cyclic loading. The model reinforcement (Figure 7b) was a polyester geogrid with strand width 1 mm, spacing between adjacent strands 18 mm, covering ratio 9.5%, and rupture tensile strength at an axial strain rate of  $1.0\%/min = 19.6 \text{ kN/m}$ .

**Earth pressure.** First, the test results when the facing bottom was hinge-supported (i.e. facing bottom condition H in Figure 9) will be discussed. Figure 26 shows two typical relations between earth pressure and facing displacement. When the backfill is reinforced with reinforcement layers connected to the facing (case R&C, Figure 26b), the earth pressure increases greatly with cyclic loading, and similarly with the unreinforced backfill (Figure 26a). The mechanism of the development of high earth pressure with lateral cyclic loading of the FHR facing is different in these two cases. When the backfill is reinforced with reinforcement connected to the FHR facing, high earth pressure develops without the formation of an active wedge because the stiffness of the backfill increases with cyclic loading, as the deformation is highly restrained by reinforcement. The relationships between the peak earth pressure coefficient,  $K_{peak}$ , and the number of loading cycles,  $N$ , are

summarised in Figures 11a and 11b. When the reinforcement is connected to an FHR facing, the facing performs as a continuous beam supported by a number of reinforcement layers (Figure 22). Therefore even the earth pressure becomes large by cyclic loading, the facing is only slightly damaged structurally, and the facing bottom is scarcely pushed out. Rather, higher earth pressure results in higher confining pressure, and therefore higher stiffness and strength of the backfill (i.e. better performance of the retaining wall).

It may also be seen from Figure 27 that, when the reinforcement is connected to the facing, the facing movement mode (either active only or active and passive equally) has no significant effect on the development of earth pressure. This trend is also seen from Figure 11a, which shows the relationships between  $K_{peak}$  in the respective cycles and the number of loading cycles,  $N$ , for  $D/H = 0.2\%$  when the backfill is reinforced with and without connection of the reinforcement to the facing. The facing displacement mode is either active only (A) or active and passive equally (A&P). Similar relationships for  $D/H = 0.2\%$  and  $0.6\%$  when the facing displacement mode is active only (A) are presented in Figure 11b. The values of  $K_{peak}$  at selected numbers of cycles for different  $D/H$  values when the backfill is reinforced while the facing displacement mode is active only (A) and the facing bottom is hinge-supported (H) are summarised in Figure 12b (reinforcement not connected to the facing) and Figure 12c (reinforcement connected to the facing). It may be seen from these figures that the increase in  $K_{peak}$  with cyclic loading increases with an increase in  $D/H$ . This trend is stronger when the backfill is unreinforced and when the backfill is reinforced without connection of the reinforcement to the facing. Conversely, this trend is much weaker when the backfill is reinforced and the reinforcement is connected to the facing. It may also be seen that when  $D/H = 0.2\%$  the earth pressure increase is largest when the backfill is reinforced without connection of the

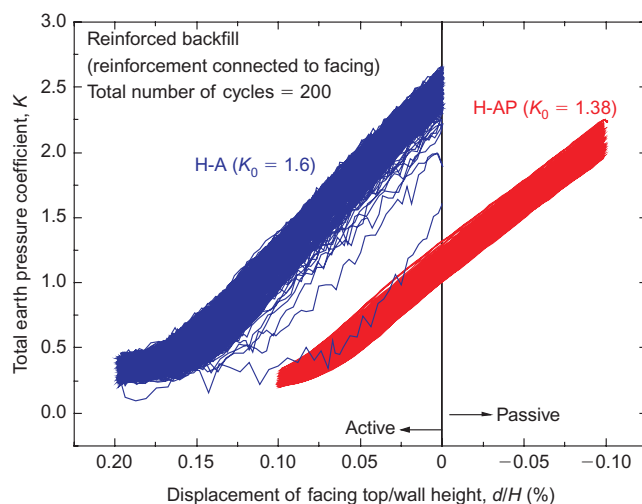


Figure 27. Effects of facing bottom displacement mode (A or AP) on the relationship between total earth pressure coefficient,  $K$ , and horizontal displacement at facing top,  $d/H$ ; reinforcement connected to facing

reinforcement to the facing (Figure 11a). This trend becomes very strong when  $D/H$  becomes 0.6% (Figure 11b). This trend can be explained as follows. Even when the backfill is reinforced, if the reinforcement is not connected to the facing, significant active failure takes place with large settlements in the backfill immediately behind the facing (Figure 28a) by the dual ratchet mechanism (Figure 15). On the other hand, the overall lateral stiffness of the whole reinforced backfill is higher than the unreinforced backfill owing to less serious active failure. Hence the increase in the passive pressure with cyclic loading by the dual ratchet mechanism becomes more significant than with the unreinforced backfill. Then the force that is necessary to push back the facing from an active state becomes larger, and greatly increased earth pressure may structurally damage the facing and/or push out the bottom of the facing. Therefore, when the facing bottom is free, an increase in the earth pressure results in significant pushing out of the bottom of the facing (Figure 28a). In this case, the earth pressure becomes smaller, as shown in Figure 19, but at the cost of a substantial increase in the backfill settlement associated with a significant active failure (Figures 28a and 28b). These results clearly indicate the importance of connecting the reinforcement to the facing.

When the reinforcement is connected to the facing,

even when the facing bottom is free, no significant active failure in the backfill takes place, as when the facing bottom is hinge-supported (Figure 29a). Therefore the settlement in the backfill does not increase noticeably, even by making the facing bottom free (Figure 29b).

*Backfill settlement.* Figure 14a presents the relationships between the backfill settlement (when  $d = 0$ ) at  $L = 5$  cm and the number of loading cycles,  $N$ , when the footing bottom is hinge-supported (H) while the backfill is reinforced, either without connection (R&No) or with connection (R&C) of the reinforcement to the facing. These data were obtained when  $D/H$  was equal to 0.2% for two different facing displacement modes: active only (A) and equally active and passive (A&P). Figure 14b compares the backfill settlements when  $D/H$  is equal to 0.2% and 0.6%. The footing bottom is hinge-supported (H) and the facing displacement mode is active only (A). The following trends of behaviour may be seen.

- The backfill settlement is largest when the backfill is not reinforced (NR), and it is smallest and nearly zero when the backfill is reinforced with reinforcement connected to the facing (R&C). This is because, when the reinforcement is connected to the facing, the confining pressure in the backfill stays

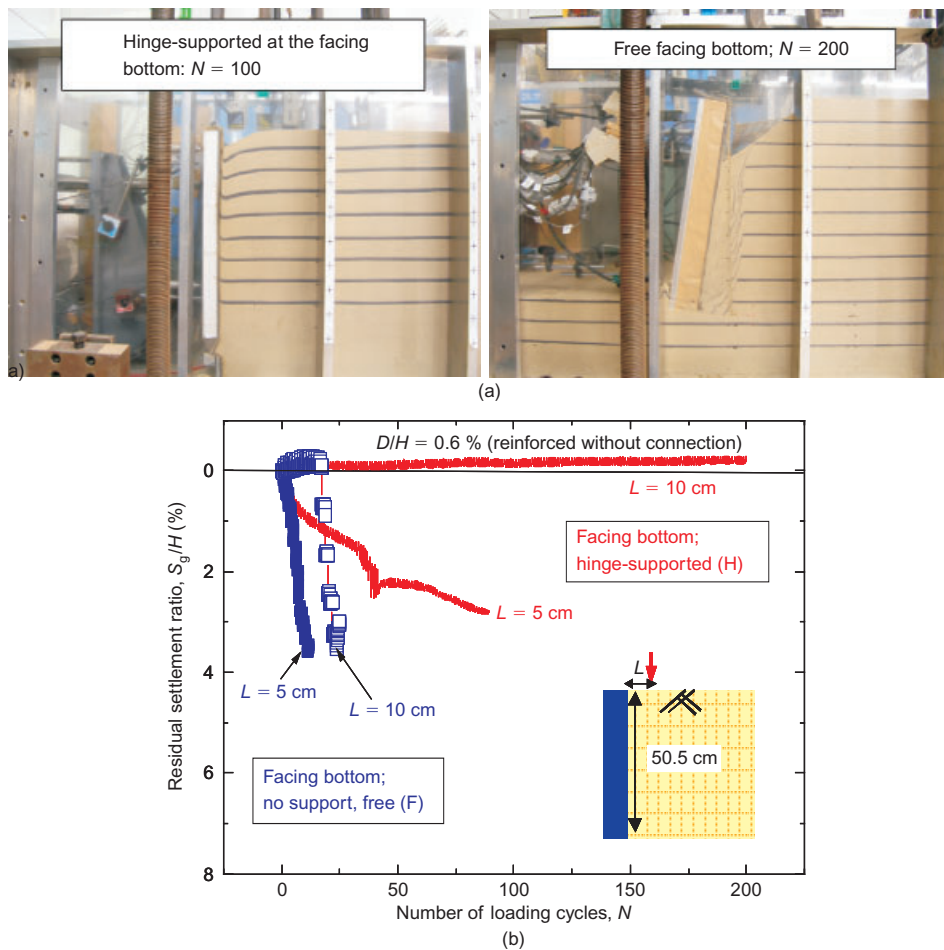


Figure 28. Effects of footing bottom condition when backfill is reinforced without connection to facing, air-dried Toyoura sand ( $D_r = 90\%$ ) and  $D/H = 0.6\%$ : (a) failure mode; (b) backfill settlement

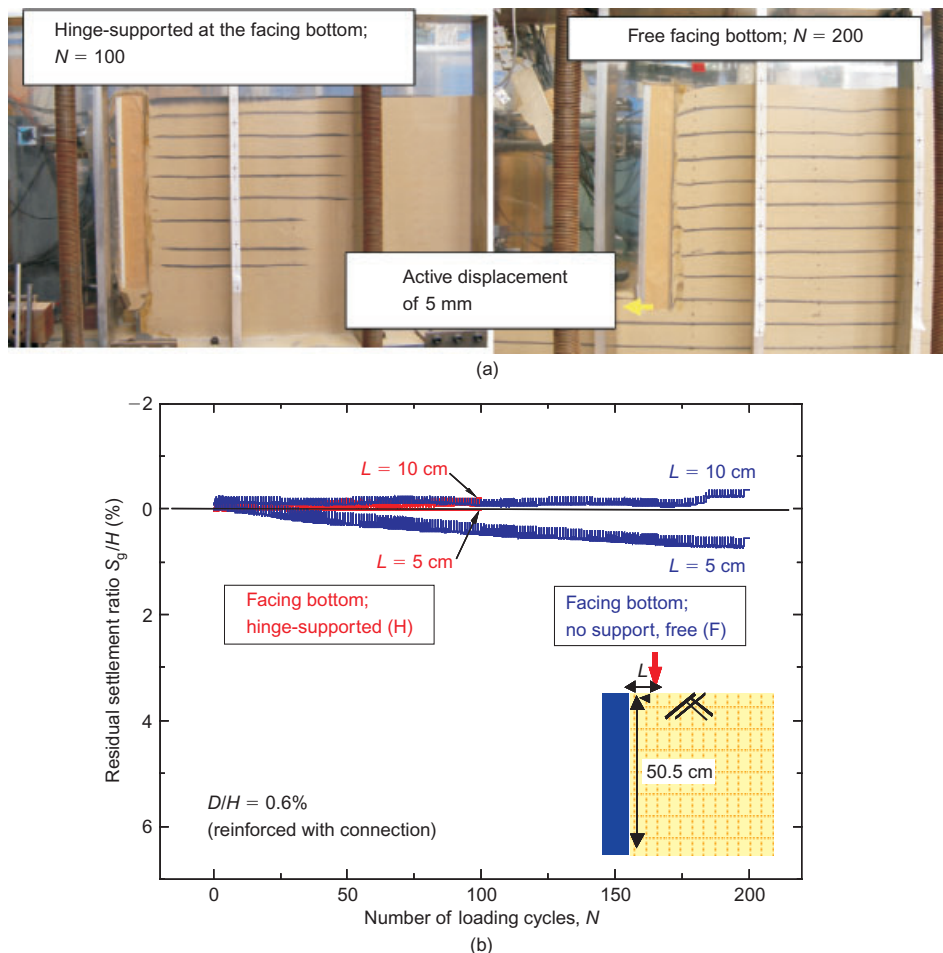


Figure 29. Effects of footing bottom condition when backfill is reinforced with connection to facing, air-dried Toyoura sand ( $D_r = 90\%$ ) and  $D/H = 0.6\%$ : (a) failure mode; (b) backfill settlement

high, which makes the backfill less deformable, and the membrane effects of the reinforcement prevent the formation of an active wedge.

- The backfill settlement is very large when the backfill is reinforced but without connection (R&No), which may not be allowable if it takes place in prototype backfill.
- The backfill settlement is larger when the facing moves only on the active side (A) than when the facing moves equally on both the active and passive sides (A&P).
- When the reinforcement is not connected to the facing, the backfill settlement immediately behind the facing is much larger when the facing bottom is free than when it is hinge-supported (Figure 28). On the other hand, when the reinforcement is connected to the facing, the backfill settlement when the facing bottom is free is very small in both cases (Figure 29).

In summary, the stability of the facing and the backfill when the facing is subjected to lateral cyclic displacements caused by seasonal thermal expansion and contraction of the girder is greatly increased by reinforcing the backfill with reinforcement connected to the facing. When the reinforcement is not connected to the facing, these advantages cannot be expected.

#### 4.3.2. Vertical cyclic loading tests

To evaluate the effect of reinforcing the backfill with geosynthetic layers on the backfill deformation caused by long-term traffic loads applied to the backfill, vertical cyclic loading tests were performed (Figure 30). Vertical cyclic load was applied to the centre of a 10 cm-wide strip footing with a rough base, placed on the backfill of air-dried Toyoura sand ( $D_r = 90\%$ ). The facing was laterally fixed, and the total lateral thrust load acting on the facing,  $L$ , was measured with a load cell arranged between the loading piston and the facing (Figure 30). The footing was allowed to rotate about a hinge at the central axis of the footing located 10 cm above the footing base. Cyclic average footing pressure in a range between 2 kPa and 17 kPa was applied at a period of 15–30 s. The other test conditions were the same as in the lateral cyclic loading tests (Figure 7).

The test results are presented in Figure 31. The backfill settlement when the backfill is unreinforced is particularly large (Figure 31a). The settlement decreases when the backfill is reinforced, whether the reinforcement is connected to the facing or not. This is because the major deformation in the backfill takes place immediately below the footing, as can be seen from the strong concentration of tensile strain in the reinforcement immediately below the footing (Figure 31c). As can be seen from Figure 31b, the

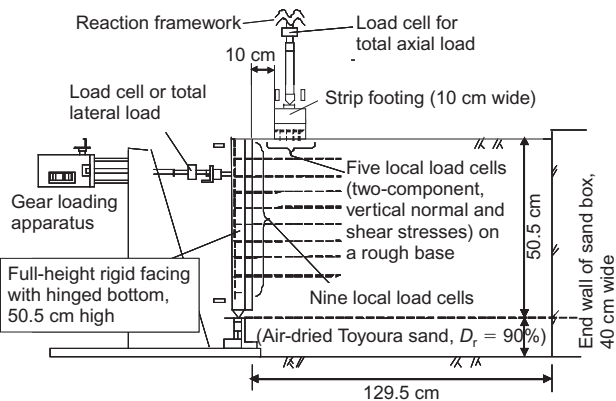


**Figure 30. Set-up of vertical cyclic loading tests (all dimensions in cm)**

lateral earth pressure on the back of the facing was initially relatively low in the unreinforced backfill (prepared by air pluviation), but it increased considerably with cyclic loading. This increased earth pressure destabilises the abutment when it is not supported laterally by a girder. When the backfill was reinforced, the lateral earth pressure, which was initially high as it was prepared by hand-

tamping, did not increase significantly with cyclic loading, whether the reinforcement was connected to the facing or not. On the other hand, the lateral thrust force activated at the facing was much higher when the reinforcement was not connected to the facing (Figure 31a). With prototype integral bridges, an increase in the lateral thrust force acting in the facing means an increase in the axial load in the girder. When the reinforcement is connected to the facing, an increase in the lateral thrust load is also resisted by the reinforcement.

These test results indicate that the detrimental effects of vertical cyclic loading by traffic on the performance of the integral bridge can be effectively prevented by reinforcing the backfill. It is very likely that the positive effects of connecting the reinforcement to the facing will become more significant when the vertical load is applied at locations closer to the facing than in these tests.

4.3.3. *Shaking-table tests*

*Models and testing methods.* Two series of shaking-table tests were performed (Aizawa et al. 2007; Hirakawa et al. 2007b; Tatsuoka et al. 2007b, 2008a, 2008b). The first series (Figure 32) compared the

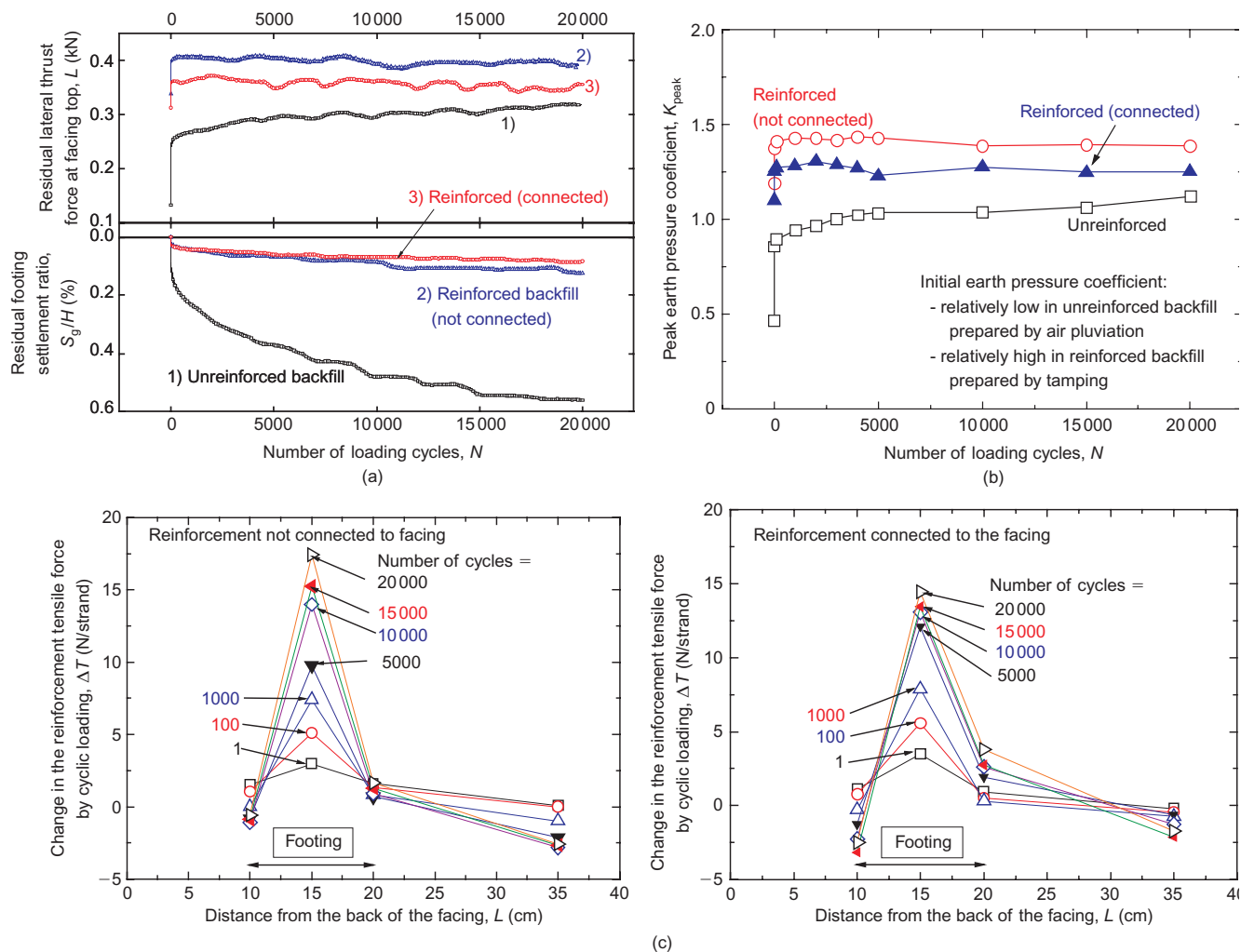


**Figure 31. Results from vertical cyclic loading tests: (a) lateral thrust force at facing top, and vertical settlement of footing; (b) earth pressure on back of facing; (c) distributions of tensile force in reinforcement**

seismic stabilities of the four models of the bridge types shown in Figure 3. Figure 33a shows the GRS integral bridge model. In all the tests, the supporting ground and the backfill were made using air-dried Toyoura sand,  $D_r = 90\%$ , by the air pluviation method. To observe the deformation of the backfill by shaking, thin horizontal layers of sand, dyed black, were placed at a vertical spacing of 10 cm immediately behind the front transparent side wall (Figure 33a). On the crest of the backfill, a surcharge of 1 kPa made of lead shots was placed to simulate the weight of the road base for railways or highways. A scale ratio of 1/10 was assumed. The abutments of the four models were made of Duralumin: all were 51 cm high and had a bottom width of 20 cm. The back and bottom faces of the abutments were made rough by gluing sand paper (no. 150). A mass of 200 kg was attached to the centre of the model girder (61 cm long) to make the equivalent length 2 m (i.e. 20 m in the assumed prototype). No pile foundation supporting the abutment was used, to examine the critical failure mode of the respective bridge types. The effects of a pile foundation and/or cement-mixing of the backfill on the dynamic stability of the integral bridge and the GRS integral bridge have been evaluated by Hirakawa *et al.* (2008) and Soma *et al.* (2008), and will be reported in the near future.

The reinforcement (Figure 33b) was a grid made of phosphor bronze consisting of 17 longitudinal strands with

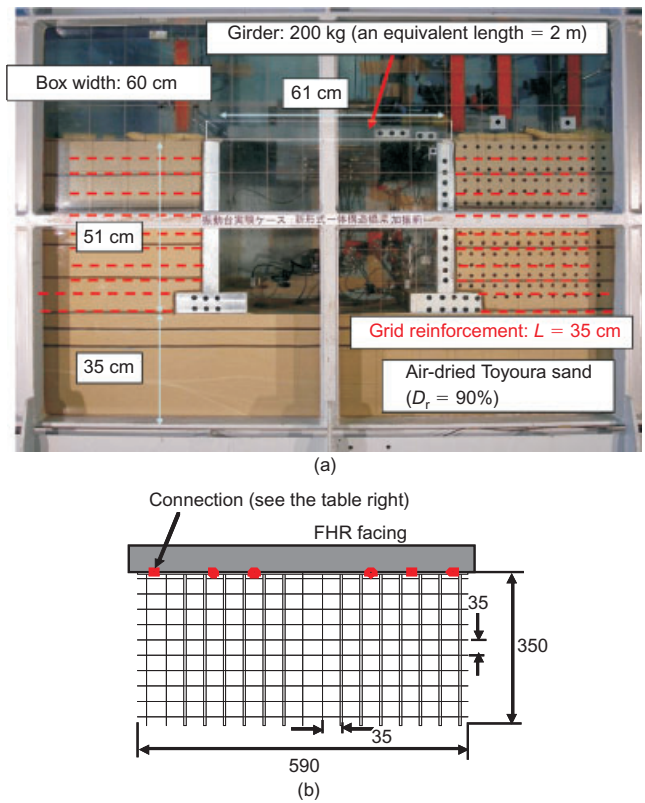


Figure 33. (a) Model of GRS integral bridge (Figure 32); (b) model reinforcement

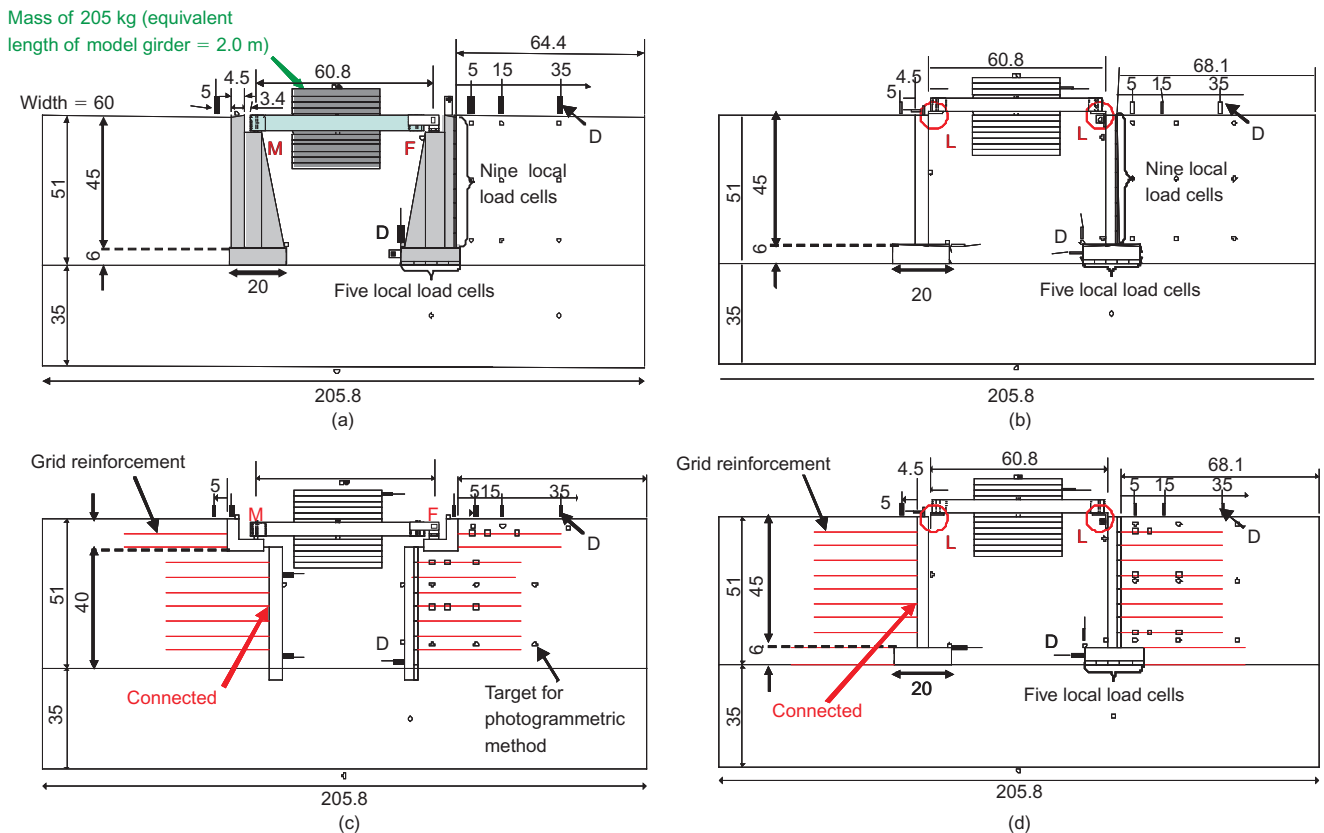


Figure 32. Models for shaking-table tests (series 1), air-dried Toyoura sand ( $D_r = 90\%$ ): (a) conventional; (b) integral; (c) GRS-RW; (d) GRS integral (Nojiri *et al.* 2006; Aizawa *et al.* 2007; Hirakawa *et al.* 2007b). D, displacement transducer; M, movable sliding support; F, fixed hinge support; L, L-shaped metal fixture (all dimensions in cm)

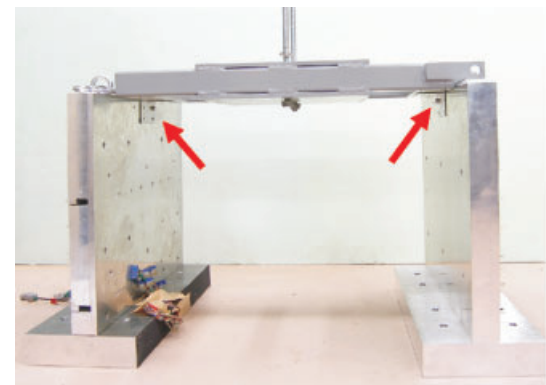
a high rupture strength, 359 N per strand. The covering ratio was 10.1%. The surface of the strands was made rough, with a friction angle of  $35^\circ$  at a confining pressure of 50 kPa, by gluing sand particles. Electric-resistance strain gauges were attached to several places of the reinforcement to measure the tensile force that developed in it. The reinforcement layers were fixed to the back of the facing by using six bolts for a facing width of 59 cm. In Figure 33a the reinforcement layers are indicated by horizontal broken lines.

For the models of the integral bridge and GRS integral bridge, the girder and facings were connected to each other with an L-shaped metal fixture (Figure 34a). The fixtures, 3 mm thick, 50 mm wide and 200 mm long, yield at a flexural angle of about  $6^\circ$ , equivalent to about 10% shear strain in the backfill (Figure 34b). This flexure occurs when the fixture supports the whole of the girder. The peak resisting moment is about 0.5 kNm, which is much smaller (by a factor of about 1/3) than the value needed to resist the moment produced by the earth pressure activated on the back of the facing when the model failed (presented in Figure 40b). Twenty sinusoidal waves at a frequency of 5 Hz were applied at the shaking table step by step increasing the maximum acceleration,  $\alpha_b$ , by increments of  $100 \text{ cm/s}^2$ .

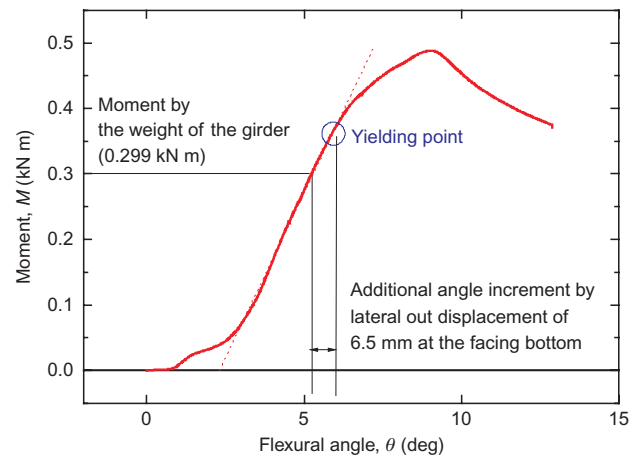
In the second series (Figure 35 and Table 1), four model tests of the GRS integral bridge were performed to evaluate the effects of the connection strength between the reinforcement and the facing. The model in test 4 is the same as the GRS integral bridge model used in the first series.

**Test results.** Figures 36a and 36b show the settlements at the crest of the backfill at 5 cm and 35 cm from the back of the facing, respectively. In Figure 36a the settlement of the sill beam of the GRS-RW bridge is presented. These values, and those presented in Figures 37 and 38, were obtained by using photographs taken after the respective shaking stages. Figure 37 shows the lateral displacements at the top and bottom of the facing. Figure 38 shows the overturning angle of the facing, and also the rotational angle of the sill beams of the GRS-RW bridge. In these figures, with the conventional and GRS-RW bridges, the displacements of the abutment and the backfill on the side supporting the girder via a fixed shoe, where all the lateral inertial force of the girder is activated, are presented. Figure 39 shows the failure models of the integral bridge and the GRS integral bridge observed after the respective tests in series 1. The following trends of behaviour may be seen from these figures.

- In series 1, the GRS integral bridge with the backfill reinforced with reinforcement connected to the facing is the most stable. The conventional type bridge, with unreinforced backfill, is the least stable.
- The stabilities of the GRS-RW bridge and the integral bridge are similar, and lie between those of the conventional bridge and the GRS integral bridge, although their failure mechanisms and modes are



(a)



(b)

**Figure 34. (a) L-shaped metal fixture; (b) its bending properties (the angle is positive when the flexure is closed;  $0.1 \text{ rad} = 5.73^\circ$ )**

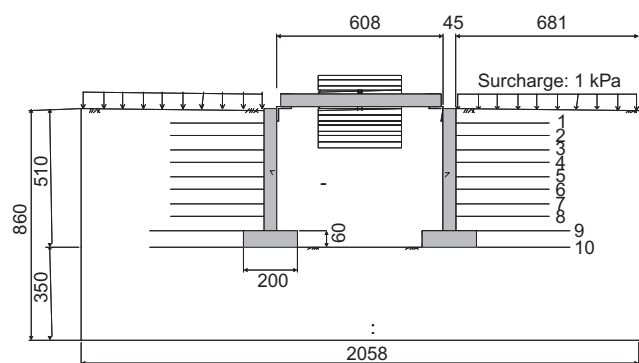


**Figure 35. Cross-section of GRS integral bridge model (tests 3 and 4 in series 2) (all dimensions in mm)**

quite different. With the GRS-RW bridge, although the retaining walls are very stable, the stability of the sill beam that supports the girder via a fixed shoe is quite low.

- The major failure mode of the integral and GRS integral bridges is outward lateral movement of the facing bottom, associated with rotation of the facing (see Figure 39). With the integral bridge, the strength of the fixture integrating the girder and the facings of the GRS integral bridge is insufficient to resist fully this mode of displacement of the facing.

**Table 1. Different conditions of model reinforcements used in the second series**

Test no.	No. of reinforcement layers	Connection conditions		Strand		Covering ratio, CR (%)	Friction angle when CR = 100% (degrees)
		Connection strength (N/layer)	Connection method	Rupture strength (N)	No. of strands		
1	8	400	Melting, 4 points	207	17	10.1	35.0
2	9	520	Bolt (M3), 4 points				
3	10	520	Bolt (M3), 4 points				
4	10	1070	Bolt (M3), 6 points				

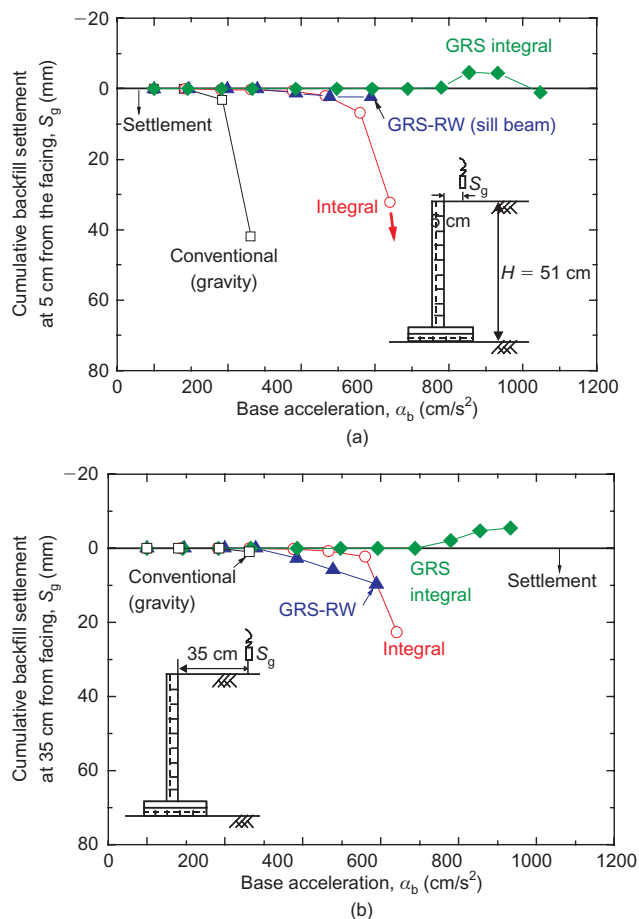


**Figure 36. Cumulative residual settlement of the backfill at (a) 5 cm and (b) 35 cm from the back of the facing, against base acceleration**

Figure 40 shows the distributions with depth of earth pressure activated by dynamic loading on the facing at the 10th cycle at each shaking stage with the GRS integral bridge (series 1). In the upper part of the facing (for a range of  $z = 0$  to about 30 cm), the largest earth pressure at the respective heights is activated when the facing top is under the passive condition, developed by the pushing-in movement of the girder into the backfill. On the other hand, in the lowest part of the facing (for a range of  $z$  larger than about 30 cm), the largest earth pressure is activated when the facing top is under the active condition, developed by the rotation of the facing associated

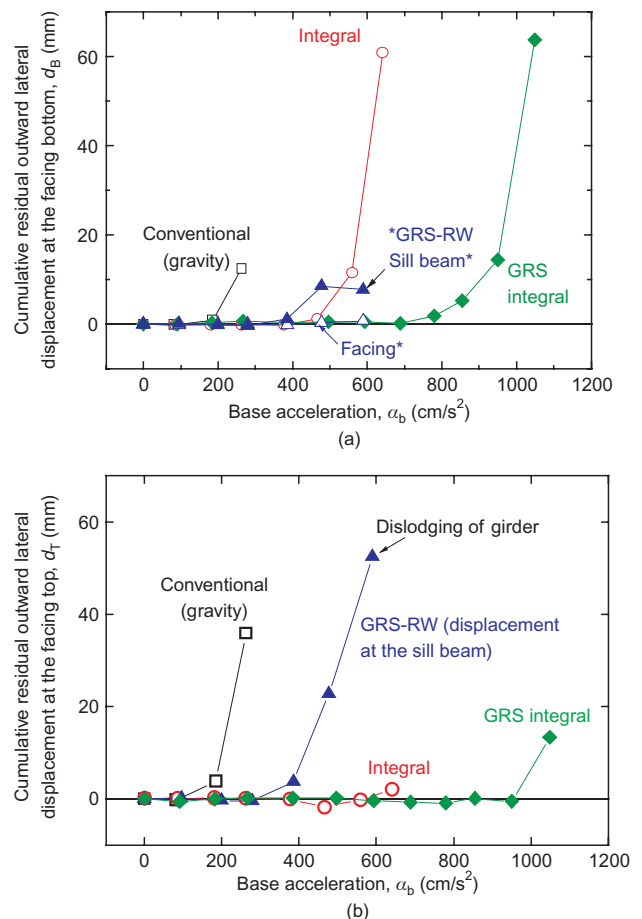


**Figure 37. Cumulative outward displacement at (a) bottom and (b) top of facing, against base acceleration**

with outward movement of the girder away from the backfill. These trends of behaviour show that the major critical displacement mode is rotation of the facing relative to the backfill (see Figure 39). In Figure 40a, the earth pressure suddenly decreases when the base acceleration increases from 950  $\text{cm/s}^2$  to 1048  $\text{cm/s}^2$ . This change is due to the start of significant failure in the backfill behind the facing associated with significant rotation of the facing relative to the backfill (Figure 39b).

The earth pressures shown in Figure 40 were obtained from the outputs of nine local load cells attached on the back of the facing (Figure 32) without having been corrected for accelerations activated in the respective load

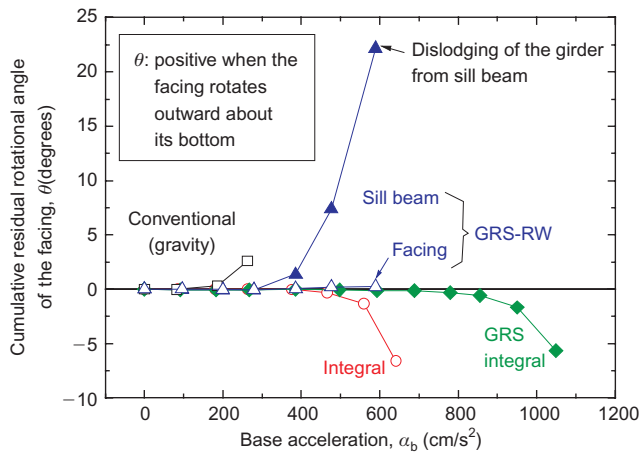


**Figure 38. Cumulative facing rotation against base acceleration**

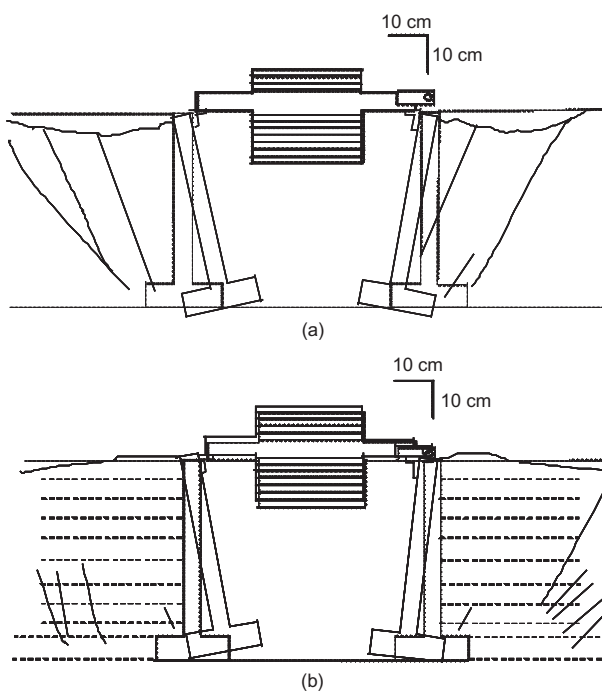


**Figure 39. Failure modes (series 1): (a) integral bridge; (b) GRS integral bridge (with high connection strength)**

cells. Probably for this reason, false slightly negative values were recorded at several places when the base acceleration became very high. For example, in Figure 40a the earth pressure at the highest level when the base acceleration was 1048 cm/s<sup>2</sup> should be close to zero, as the backfill at this level did not show any significant resistance against the pushing-in movement of the girder. However, this error is insignificant.

Figure 41 shows the effects of the number of reinforcement layers and the connection strength on the dynamic behaviour of the GRS integral bridge from test series 2 (Table 1). In this figure, the behaviour when the backfill is unreinforced (i.e. the integral bridge) is also shown for reference. Figure 42 shows the maximum tensile force measured at representative places of the reinforcement in test 4 (i.e. the GRS integral bridge in series 1). The

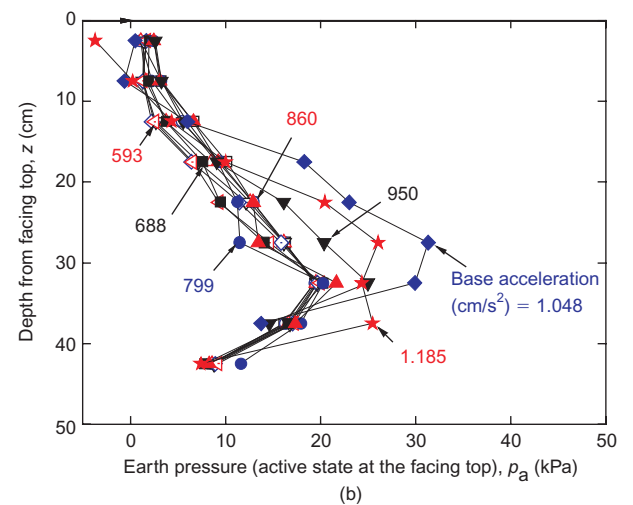
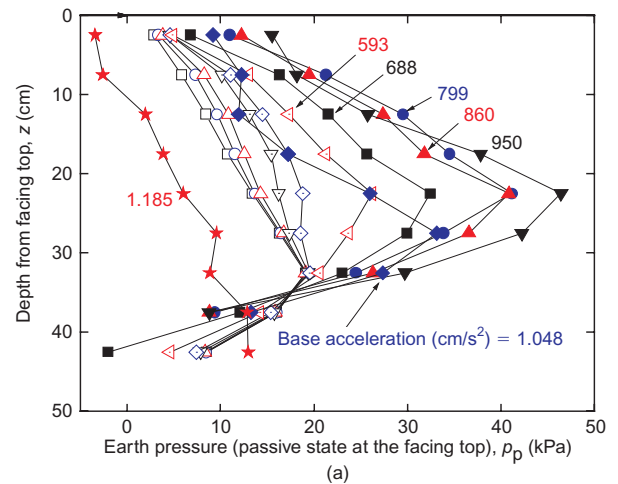


**Figure 40. Earth pressure distribution with depth on the facing at 10th cycle at each stage (numbers indicate acceleration at shaking table), GRS integral bridge: (a) passive; (b) active state at facing top**

following trends of behaviour may be seen from these figures.

- The stability increases with an increase in the connection strength between the reinforcement and the facing, and with the number of reinforcement layers.
- The connection strength at the lower part of the facing controls the dynamic stability of the GRS integral bridge: in test 4 the tensile force immediately behind the facing in the reinforcement layer near the facing bottom becomes very high, which is due to the rotational displacements of the facing relative to the backfill when the facing top is under the passive state.

With unreinforced backfill, the dual ratchet mechanism (Figure 15) becomes active by cyclic relative lateral displacements between the facing and the backfill during dynamic loading. The passive earth pressure increased by this mechanism (Figure 40a), which pushed out the facing bottom (Figure 37), and thus increased the settlement of

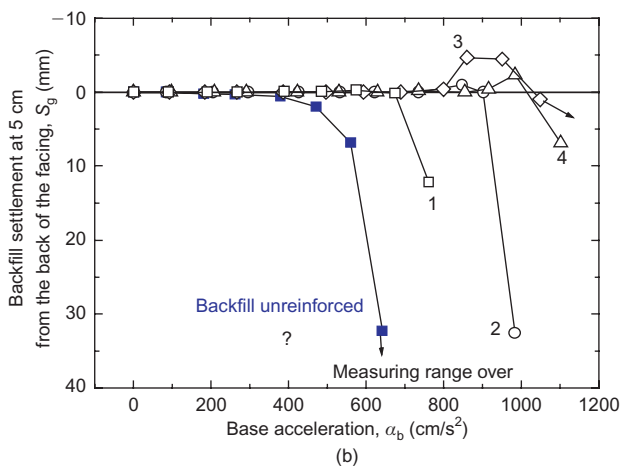
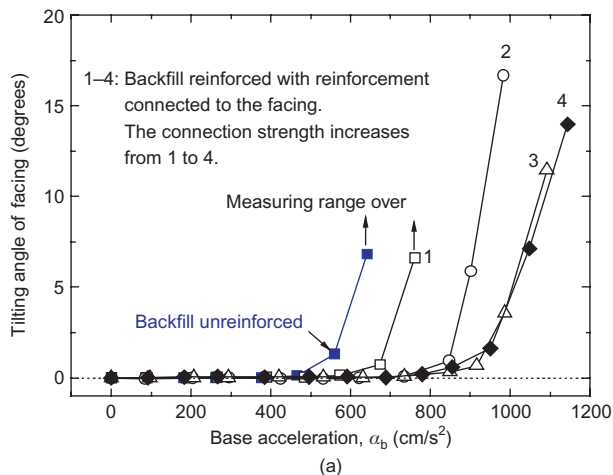


Figure 41. Effects on: (a) residual tilting angle of facing; (b) residual settlement of backfill crest (5 cm from back of facing) (series 2)

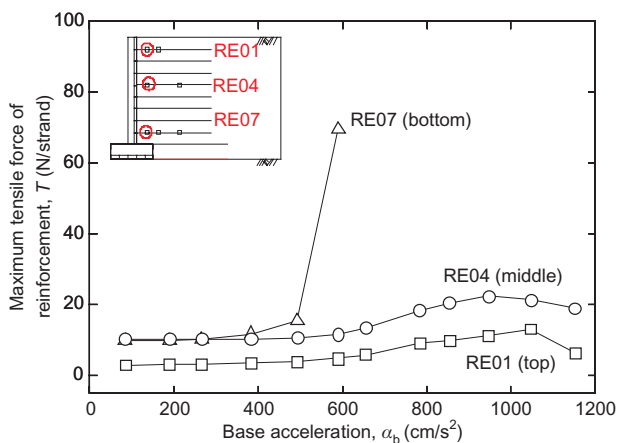


Figure 42. Relationship between tensile force of reinforcement and base acceleration, GRS integral bridge (series 1, and test 4 in series 2)

the backfill associated with the active failure (Figure 36). This trend can also be seen from Figure 39a. This test result also indicates that reinforcing the backfill with reinforcement layers firmly connected to the facing with high connection strength is essential for a high seismic stability of integral bridge.

### 5. SUMMARY AND DISCUSSIONS

Figure 43 summarises the load and resistance components for the facing rotation relative to the backfill for GRS integral bridges, as derived from the test results presented above. The two major resisting components are the passive pressure in the upper part of the backfill, and the tensile force of the reinforcement at the lower part of the facing. The former can be increased by lightly cement-mixing the relevant part of the backfill. The latter is the minimum value among the connection strength, the tensile rupture strength of the reinforcement, and the pullout strength of the reinforcement. Therefore all of these resisting components should be made sufficiently high. Further study is necessary in this respect.

Another type of integral bridge type has been proposed that places an EPS geofoam block between the RC abutment and the geosynthetic-reinforced backfill to reduce the lateral earth pressure developed (Horvath 2005). This type of bridge does not have the benefits conferred by connecting the reinforcement layers to the RC abutment. A similar type of bridge, but with a void between the RC abutment and the reinforced backfill rather than an EPS geofoam block, has the same drawbacks as above.

With conventional bridges (Figure 1) and GRS-RW bridges (Figure 3b), the length of a single simply supported girder is restricted to avoid excessive lateral load being activated on the abutment on which the fixed shoe supports the girder. With integral bridges (Figure 4), the girder length is limited to avoid excessive large cyclic lateral displacements at the top of the abutments by seasonal thermal expansion and contraction of the girder. The girder length is also restricted to limit the lateral seismic load activated on the abutments. With the GRS integral bridge, such restrictions are less severe. With GRS integral bridges, the actual length of the girder relative to the abutment height can generally be much greater than that depicted in Figure 6.

Figure 44 compares the characteristic features of the four different bridge types described in the preceding sections. The rating shown in this figure is only an approximation. The full points allocated to each item are three, and these are reduced by one when any of the negative factors A–G listed below the table applies. The horizontal accelerations at which the respective bridge models collapsed in the shaking-table tests (i.e. series 1 explained above) are listed in the second column from the right. A total of nine points is given only to the GRS integral bridge.

### 6. CONCLUSIONS

A new type of bridge, the GRS integral bridge, is proposed, which comprises an integral bridge and geosynthetic-reinforced backfill. The model tests indicate that GRS integral bridges:

- exhibit essentially zero settlement in the backfill and no structural damage to the facing from an increase in the lateral earth pressure when subjected to lateral

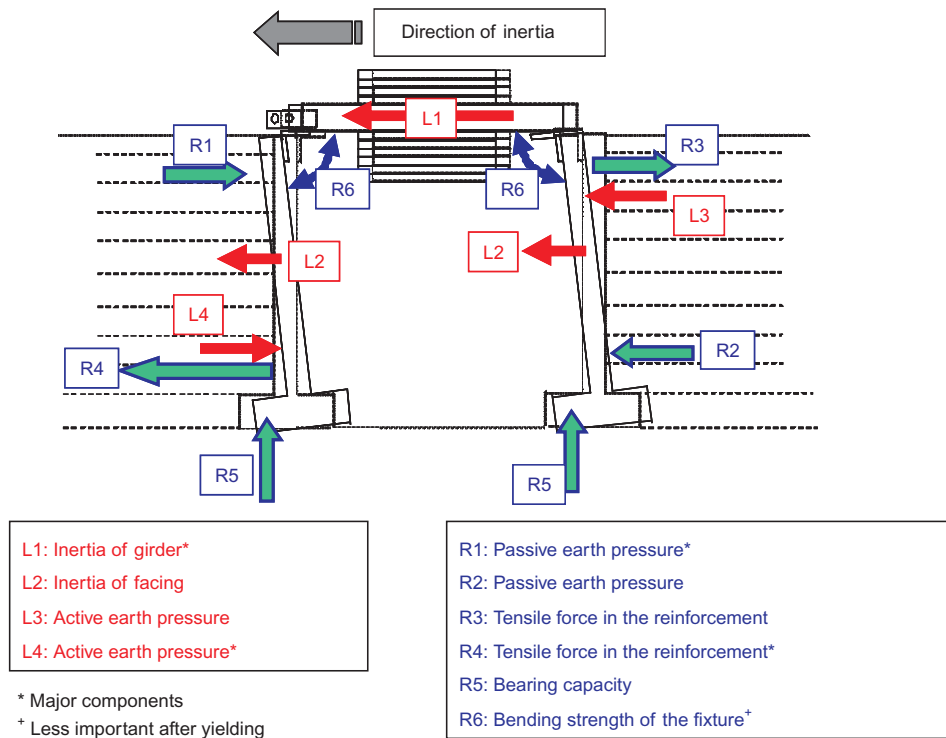
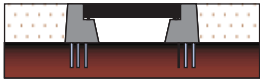
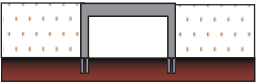


Figure 43. Load and resistance components for facing rotation, GRS integral bridge

Bridge type	Cost & period of construction	Maintenance cost	Seismic stability	Total
 Conventional	1 A, B	1 C, D	1 F, G 252 gal*	3
 Integral	2 B	1 D, E	2 F 641 gal*	5
 GRS RW	3	1 C, D'	2 G' 589 gal*	6
 GRS Integral	3	3	3 1048 gal*	9

(\* Failure acceleration in model shaking table tests)

- A = needs for massive abutments because of cantilever structure.
- B = needs for piles because of cantilever-structural type abutments and construction of backfill after piles and abutments.
- C = high cost for construction and long-term maintenance of girder shoes (i.e. bearings) and low seismic stability.
- D = long-term backfill settlement by self-weight and traffic loads.
- D' = long-term settlement of sill beam.
- E = cyclic lateral displacements of abutment top caused by thermal expansion and contraction of girder, resulting in high earth pressure and large backfill settlement.
- F = large backfill settlement and large dynamic earth pressure.
- G = low seismic stability due to independent performance of two abutments.
- G' = low seismic stability of the sill beam.

Figure 44. Rating of different bridge types based on cost and performance

cyclic displacements at the top of the facing caused by thermal cyclic expansion and contraction of the girder; and

- have a very high seismic stability of both structural components (the pair of abutments and the girder) and backfill, because they are integrated with each other.

These characteristic features are due to the following:

- Shoes (bearings) are not used to support the girder.
- The girder is continuous.
- The backfill is reinforced with geogrid layers firmly connected to the facing.
- Full-height rigid facings (i.e. bridge abutments) are stage-constructed after the construction of the full-height geosynthetic-reinforced backfill and pile foundations (if needed).

Staged construction means that pile foundations, if needed, are much lighter than with conventional bridges and integral bridges. The GRS integral bridge is therefore highly cost-effective in construction and long-term maintenance, while remaining very stable under static and seismic loading conditions.

## ACKNOWLEDGEMENTS

The study was financially supported by the Ministry of Education, Culture, Sports, Science and Technology, the Japanese government, the Japan Society for the Promotion of Science, the Tokyo University of Science, and the Railway Technical Research Institute, Japan. The authors thank all their previous and current colleagues for their help.

## NOTATIONS

Basic SI units are given in parentheses.

$b$	distance from back of facing (m)
$D$	double amplitude of lateral displacement of facing top (m)
$D_r$	relative density (dimensionless)
$d$	displacement at top of facing (positive for active displacement) (m)
$d_T, d_B$	displacements at top and bottom of facing (positive for active displacement) (m)
$H$	wall height (m)
$K$	total earth pressure coefficient (dimensionless)
$K_0$	coefficient of earth pressure at rest (dimensionless)
$K_{peak}$	peak total earth pressure coefficient in each cycle (dimensionless)
$L$	distance from the back of facing at backfill crest (m)
$L_t$	residual lateral thrust force at facing top (N)
$M$	moment (Nm)
$N$	number of loading cycles (dimensionless)
$p_a$	active earth pressure (Pa)

$p_p$	passive earth pressure (Pa)
$Q$	total earth force per width of facing (N)
$S_g$	settlement at backfill crest (m)
$t$	elapsed time (s)
$T_{peak}$	peak tensile force per strand of reinforcement in each cycle (N)
$z$	depth from facing top (m)
$\alpha$	peak lateral acceleration at the shaking table ( $m/s^2$ )
$\Delta T$	change in reinforcement tensile force by cyclic loading per strand (N)
$\gamma$	total unit weight of backfill ( $N/m^3$ )
$\delta$	cumulative residual rotation angle at facing (degree)
$\theta$	flexural angle (degree)

## REFERENCES

- Abu-Hejleh, N., Zornberg, J. G., Wang, T. & Watcharamonthein, J. (2002). Monitored displacements of unique geosynthetic-reinforced soil bridge abutments. *Geosynthetics International*, **9**, No. 1, 71–95.
- Aizawa, H., Nojiri, M., Hirakawa, D., Nishikiori, H., Tatsuoka, F., Tateyama, M. & Watanabe, K. (2007). Validation of high seismic stability of a new type integral bridge consisting of geosynthetic-reinforced soil walls. *Proceedings of the 5th International Symposium on Earth Reinforcement (IS Kyushu 2007)*, pp. 819–825.
- El-Emam, M. M. & Bathurst, R. J. (2005). Facing contribution to seismic response of reduced-scale reinforced soil walls. *Geosynthetics International*, **12**, No. 5, 215–238.
- England, G. L., Neil, C. M. & Bush, D. I. (2000). *Integral Bridges: A Fundamental Approach to the Time-Temperature Loading Problem*, Thomas Telford, London.
- Fakharian, K. and Attar, I. H. (2007). Static and seismic numerical modeling of geosynthetic-reinforced soil segmental bridge abutments. *Geosynthetics International*, **14**, No. 4, 228–243.
- Hirakawa, D., Nojiri, M., Aizawa, H., Tatsuoka, F., Sumiyoshi, T. & Uchimura, T. (2006). Behaviour of geosynthetic-reinforced soil retaining wall subjected to forced cyclic horizontal displacement at wall face. *Proceedings of the 8th International Conference on Geosynthetics*, Yokohama, Vol. 3, pp. 1075–1078.
- Hirakawa, D., Nojiri, M., Aizawa, H., Tatsuoka, F., Sumiyoshi, T. & Uchimura, T. (2007a). Residual earth pressure on a retaining wall with sand backfill subjected to forced cyclic lateral displacements. *Soil Stress–Strain Behavior: Measurement, Modeling and Analysis*, Ling, H. I., Callisto, L., Leshchinsky, D. and Koseki, J., Editors, Springer, pp. 865–874.
- Hirakawa, D., Nojiri, M., Aizawa, H., Nishikiori, H., Tatsuoka, F., Tateyama, M. & Watanabe, K. (2007b). Effects of the tensile resistance of reinforcement embedded in the backfill on the seismic stability of GRS integral bridge. *Proceedings of the 5th International Symposium on Earth Reinforcement (IS Kyushu 2007)*, pp. 811–817.
- Hirakawa, D., Tatsuoka, F., Aizawa, H., Nishikiori, H., Soma, R. and Sonoda, Y. (2008). Effects of piles on the stability of geosynthetic-reinforced soil integral bridge. *Proceedings of the 43rd Japanese National Conference on Geotechnical Engineering*, Hiroshima, pp. 1543–1544 (in Japanese).
- Horvath, J. S. (2005). Integral-abutment bridges: geotechnical problems and solutions using geosynthetics and ground improvement. *Proceedings of the 2005 FHWA Conference on Integral Abutment and Jointless Bridges*, Baltimore, MD, USA, pp. 281–291.
- Huang, C.-C. & Wu, S.-H. (2007). Simplified approach for assessing seismic displacements of soil-retaining walls. Part II: Geosynthetic-reinforced walls with rigid panel facing. *Geosynthetics International*, **14**, No. 5, 264–276.
- Koseki, J., Bathurst, R. J., Guler, E., Kuwano, J. & Maugeri, M. (2006).

- Seismic stability of reinforced soil walls. *Proceedings of the 8th International Conference on Geosynthetics*, Yokohama, Vol. 1, pp. 51–77.
- Murata, O., Tateyama, M. & Tatsuoka, F. (1994). Shaking table tests on a large geosynthetic-reinforced soil retaining wall model. *Proceedings of the International Symposium on Recent Case Histories of Permanent Geosynthetic-Reinforced Soil Retaining Walls*, Tatsuoka, F., and Leshchinsky, D., Editors, Balkema, pp. 259–264.
- Nakarai, K., Uchimura, T., Tatsuoka, F., Shinoda, M., Watanabe, K. & Tateyama, M. (2002). Seismic stability of geosynthetic-reinforced soil bridge abutment. *Proceedings of the 7th International Conference on Geosynthetics*, Nice, Vol. 1, pp. 249–252.
- Ng, C., Springman, S. & Norrish, A. (1998). Soil–structure interaction of spread-base integral bridge abutments. *Soils and Foundations*, **38**, No. 1, 145–162.
- Nojiri, M., Aizawa, H., Hirakawa, D., Nishikiori, H., Tatsuoka, F., Tateyama, M. & Watanabe, K. (2006). Evaluation of dynamic failure modes of various bridge types by shaking table tests. *Geosynthetics Engineering Journal*, **21**, 159–166 (in Japanese).
- Shinoda, M., Uchimura, T. & Tatsuoka, F. (2003a). Increasing the stiffness of mechanically reinforced backfill by preloading and prestressing. *Soils and Foundations*, **43**, No. 1, 75–92.
- Shinoda, M., Uchimura, T. & Tatsuoka, F. (2003b). Improving the dynamic performance of preloaded and prestressed mechanically reinforced backfill by using a ratchet connection. *Soils and Foundations*, **43**, No. 2, 33–54.
- Soma, R., Sonoda, Y., Aizawa, H., Nishikiori, H., Tatsuoka, F. & Hirakawa, D. (2008). Effects of cement-stabilization of the backfill on seismic performance of GRS integral bridge. *Proceedings of the 43rd Japanese National Conference on Geotechnical Engineering*, Hiroshima, pp. 1547–1548 (in Japanese).
- Tatsuoka, F. (1992). Roles of facing rigidity in soil reinforcing. Keynote Lecture. *Proceedings of the International Symposium on Earth Reinforcement Practice, IS-Kyushu '92*, Vol. 2, pp. 831–870.
- Tatsuoka, F. (2004). Cement-mixed soil for Trans-Tokyo Bay Highway and railway bridge abutments. *Proceedings of GeoTrans 04*, Los Angeles, ASCE GSP No. 126, pp.18–76.
- Tatsuoka, F., Tateyama, M., Uchimura, T. & Koseki, J. (1997). Geosynthetic-reinforced soil retaining walls as important permanent structures. *Geosynthetics International*, **4**, No. 2, 81–136.
- Tatsuoka, F., Koseki, J., Tateyama, M., Munaf, Y. & Horii, N. (1998). Seismic stability against high seismic loads of geosynthetic-reinforced soil retaining structures. Keynote Lecture. *Proceedings of the 6th International Conference on Geosynthetics*, Atlanta, Vol. 1, pp. 103–142.
- Tatsuoka, F., Masuda, T. & Siddiquee, M. S. A. (2003). Modelling the stress–strain behaviour of sand in cyclic plane strain loading. *Journal of Geotechnical and Environmental Engineering, ASCE*, **129**, No. 6, 450–467.
- Tatsuoka, F., Tateyama, M., Aoki, H. & Watanabe, K. (2005). Bridge abutment made of cement-mixed gravel backfill. *Ground Improvement: Case Histories*, Indradratna, B. and Chu, J., Editors, Elsevier Geo-Engineering Book Series, Vol. 3, pp. 829–873.
- Tatsuoka, F., Tateyama, M., Mohri, Y. & Matsushima, K. (2007a). Remedial treatment of soil structures using geosynthetic-reinforcing technology. *Geotextiles and Geomembranes*, **25**, Nos. 4/5, 204–220.
- Tatsuoka, F., Hirakawa, D., Nojiri, M., Aizawa, H., Tateyama, M. & Watanabe, K. (2007b). A new type integral bridge comprising of geosynthetic-reinforced soil walls. *Proceedings of the 5th International Symposium on Earth Reinforcement (IS Kyushu 2007)*, pp. 803–809.
- Tatsuoka, F., Hirakawa, D., Nojiri, M., Aizawa, H., Tateyama, M. & Watanabe, K. (2008a). integral bridge with geosynthetic-reinforced backfill. *Proceedings of the First Pan American Geosynthetics Conference & Exhibition*, Cancun, pp. 1199–1208.
- Tatsuoka, F., Hirakawa, D., Aizawa, H., Nishikiori, H., Soma, R. & Sonoda, Y. (2008b). Importance of strong connection between geosynthetic reinforcement and facing for GRS integral bridge. *Proceedings of the 4th International Conference on Geosynthetics*, Shanghai, pp. 205–210.
- Uchimura, T., Tateyama, M., Koga, T. & Tatsuoka, F. (2003a). Performance of a preloaded-prestressed geogrid-reinforced soil pier for a railway bridge. *Soils and Foundations*, **43**, No. 6, 33–50.
- Uchimura, T., Tatsuoka, F. & Nakarai, K. (2003b). Seismic stability of preloaded and prestressed reinforced soil abutments. *Proceedings of the 12th Asian Regional Conference on Soil Mechanics and Foundation Engineering*, Singapore, Vol.1, pp. 339–342.
- Uchimura, T., Tamura, Y., Tateyama, M., Tanaka, I. & Tatsuoka, F. (2005). Vertical and horizontal loading tests on full-scale preloaded and prestressed geogrid-reinforced soil structures. *Soils and Foundations*, **45**, No. 6, 65–74.
- Watanabe, K., Tateyama, M., Yonezawa, T., Aoki, H., Tatsuoka, F. & Koseki, J. (2002). Shaking table tests on a new type bridge abutment with geogrid-reinforced cement treated backfill. *Proceedings of the 7th International Conference on Geosynthetics*, Nice, Vol. 1, pp. 119–122.

**The Editor welcomes discussion on all papers published in *Geosynthetics International*. Please email your contribution to [discussion@geosynthetics-international.com](mailto:discussion@geosynthetics-international.com) by 15 February 2010.**